(12)

Technical Summary

Seismic Discrimination

30 September 1980

Prepared for the Defense Advanced Research Projects Agency
Nuclear Monitoring Research Office under Contract F19628-80-C-0002 by

Lincoln Laboratory
MASSACHUSETTS INSTITUTE OF TECHNOLOGY
LEXINGTON, MASSACHUSETTS

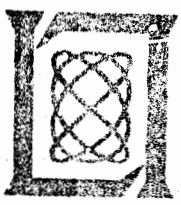

The work reported in this document was performed at Lincoln Laboratory, a center for research operated by Massachusetts Institute of Technology. This work is a part of Project Vela Uniform, which is sponsored by the Advanced Research Projects Agency under Air Force Contract [illegible] (ARPA Order 512).

This report may be reproduced to satisfy needs of U.S. Government agencies.

This technical report has been reviewed and is approved for publication.

FOR THE COMMANDER

Raymond L. Loiselle, Lt. Col., USAF
Chief, ESD Lincoln Laboratory Project Office

Non-Lincoln Recipients

PLEASE DO NOT RETURN

Permission is given to destroy this document when it is no longer needed.

DISCLAIMER NOTICE

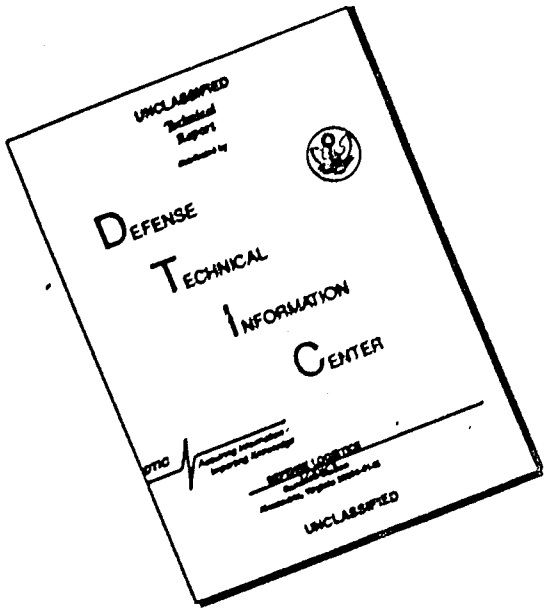

THIS DOCUMENT IS BEST QUALITY AVAILABLE. THE COPY FURNISHED TO DTIC CONTAINED A SIGNIFICANT NUMBER OF PAGES WHICH DO NOT REPRODUCE LEGIBLY.

MASSACHUSETTS INSTITUTE OF TECHNOLOGY

LINCOLN LABORATORY

SEISMIC DISCRIMINATION

SEMIANNUAL TECHNICAL SUMMARY REPORT
TO THE
DEFENSE ADVANCED RESEARCH PROJECTS AGENCY

1 APRIL – 30 SEPTEMBER 1980

ISSUED 2 MARCH 1981

LEXINGTON MASSACHUSETTS

ABSTRACT

This Semiannual Technical Summary describes the Lincoln Laboratory Vela Uniform program for the period 1 April to 30 September 1980. Section I describes progress in the development of a prototype Seismic Data Center. During this report period, advances have been made in three important subsystems: the Seismic Analysis Station, the Local Computer Network, and the Data Base Management System. Section II describes a series of studies into the seismic processing algorithms to be used at the Seismic Data Center. The results of several investigations in General Seismology are included in Sec. III.

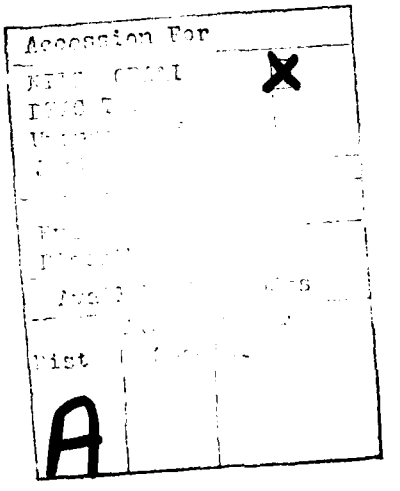

CONTENTS

SUMMARY

This is the thirty-third Semiannual Technical Summary (SATS) report describing the activities of Lincoln Laboratory funded under Project Vela Uniform. This report covers the period 1 April to 30 September 1980. Project Vela Uniform is a program of research into the discrimination between earthquakes and nuclear explosions by seismic means. An important recent emphasis of the project is in the development of data-handling and analysis techniques that may be appropriate for the monitoring of a potential Comprehensive Test Ban Treaty, presently under negotiation. During FY 1979, Lincoln Laboratory completed a design for a Seismic Data Center (SDC) that would satisfy this requirement, and the FY 1980 program consists of beginning the development of a prototype SDC which will test and refine the various design concepts. Along with this development, seismic research is continuing, with emphasis on those areas directly related to the operations of the SDC.

To date, the Lincoln Laboratory program has focused on three of the most important subsystems of the prototype SDC: the Seismic Analysis Station (SAS), the Local Computer Network, and the Data Base Management System. Hardware acquisition for the SAS has been essentially completed, and efforts in this area have been focused on the development of a responsive waveform display which will include a smooth scrolling capability. Hardware for the prototype Data Base Management System is on order, but has not yet been received. Efforts in this area have concentrated on the development of a modification to the kernel of the UNIX operating system that will permit rapid data transfer. The modified system, TUNE, is nearing completion and may be utilized in the SAS. The Local Computer Network is being developed to our specifications by a subcontractor. Interactions with this subcontractor lead us to believe that the design of this subsystem is progressing well, and we anticipate delivery of the subsystem on schedule.

Research into the algorithms that will form the basis for seismic processing at the SDC has continued in several areas. On the basis of their spectral characteristics, it appears possible to identify local signals automatically with a high degree of success. A set of synthetic arrivals has been used to evaluate some existing automatic association algorithms. There is a substantial gap between the performance of these algorithms and the much better performance of a human analyst, but future research is expected to reduce this difference. Evidence is given that it may be necessary to routinely use master-event techniques for earthquake location in regions of strong lateral inhomogeneity, such as island areas. We have examined some of the difficulties involved in the identification of short-period depth phases, and show that useful information can be obtained from long-period body-wave records when they are available.

Research in general seismology includes a study of the anomalous Rayleigh waves emitted by certain events at the Eastern Kazakh test site. The characteristics of these surface waves can be explained on the basis of a combined explosion/thrust faulting mechanism. A series of investigations have been carried out into the direct inversion of waveform data to obtain information about the velocity and attenuation structure of the Earth. Initial experiments have used mantle waves of long period, and results using both synthetic and real data show distinct promise. Involved in this study (and many others) is the computation of an average path-dispersion characteristic for a surface-wave path that traverses several different provinces. Analysis of this problem shows that computation of this path average, at least in certain cases, should not be based on simple geometrical path lengths in each region, but should use some additional parameters which may be computed.

M. A. Chinnery

SEISMIC DISCRIMINATION

I. SEISMIC DATA CENTER DEVELOPMENT

A. PROGRESS IN SEISMIC DATA CENTER DEVELOPMENT

During the period covered by this report, development has continued on the various subsystems (described in an earlier report[1]) of the prototype Seismic Data Center (SDC). The main emphasis of the program has been on hardware acquisition, and the development of basic systems software.

Hardware acquisition for the Seismic Analysis Station (SAS) has been essentially completed, and efforts in this area have been focused on the development of a responsive waveform display which will include a smooth scrolling capability.

Hardware for the prototype Data Base Management System is on order, but has not yet been received. Efforts in this area have concentrated on the development of a modification to the kernel of the UNIX operating system that will permit rapid data transfer. The modified system, TUNE, is nearing completion, and may be utilized in the SAS.

The Local Computer Network is being developed to our specifications by a subcontractor. Interactions with this subcontractor lead us to believe that the design of this subsystem is progressing well, and we anticipate delivery of the subsystem on schedule.

Activity concerning the communications interface has been limited to continuing discussions with DOE concerning data formats and data-transmission methods. Until these questions are resolved, work on this subsystem cannot begin.

We are conscious of the necessity to include adequate services and support for the research community. Efforts are currently under way to formulate the requirements of this community. Discussions have been held with various individual seismologists and with the Panel on Data Problems in Seismology of the National Academy of Sciences.

M. A. Chinnery
A. G. Gann

B. SEISMIC ANALYSIS STATION ARCHITECTURE

The Seismic Analysis Station (SAS) is a subsystem of the Seismic Analysis Center. It will be the focus of seismic interactive analysis for the system, providing facilities for the analyst to scan, classify, and make measurements on large amounts of seismic waveform data. This section will describe our current thoughts about the SAS architecture. Later sections summarize our work on two prototype SAS systems: Mod 1, a system for analyzing parametric data which is basically operational; and Mod 2, a waveform display system which is now partially implemented.

1. Basic Philosophy of the SAS

Our goal is to design a system which is flexible enough so that operators, within limits, can tailor the system to their needs. We also need a system which, as we learn about better methods of seismic analysis, we can easily change.

We will try to make the processes which implement the functionality required very fine grained, with simple interfaces. There will then be much interprocess communication, which

UNIX does not support efficiently. This will require a new service – efficient interprocess communication. We plan to use the TUNE kernel, now being written for the waveform database, as a basis for implementation of this function.

In addition, certain functions, whose operations are very obvious to the operators, must be very very fast. Waveform scrolling must be fast and smooth. Changes to the parametric database must quickly appear on the relevant display. This criterion may, at times, be in opposition to the idea of fine-grained processes. Any functions which are to be fast must be carefully designed; if they are monolithic, they still must be logically internally fragmented.

2. Major Software Subsystems

The divisions of software components, as we now see them, are:

- User Interface
  - Keyboard control
  - Process direction
- Interprocess Communication and Control
- Seismic and Other Applications
- Local Database
  - Parametric
  - Waveform
- Parametric Display
- Graphics Display
  - Waveform
  - General
  - Graphics supervisor
- "Analog" Control
  - Joystick
  - Data tablet
  - Knob box
  - Voice data entry system
- Network Interface
- UNIX Modifications
  - Interprocess communication
  - Scheduler
  - Disk I/O
  - Interface to TUNE kernel

The major thrust of this exercise was to separate the functional components of the system. Note that if implementation is carried out following the lines of these divisions, the operator's input and display devices would be logically separated from each other and from the computational processes which use them. This is similar to the UNIX philosophy of allowing the data to flow between processes by way of the standard input and output. One advantage of this scheme would be that display processes could be divorced from any particular input control. For example, to indicate a particular line on the parametric display, some operators might want to use the keyboard cursors, while others, the joystick.

This also allows us to experiment with the user interface. We can easily provide different faces to the users with the same internal functionality.

There might be exceptions to this philosophy of loose coupling of the processes and devices; e.g., the waveform display, because of speed considerations, might have to be more tightly coupled to its input and generating process.

The next two sections deal with two key components of the system. Interprocess communication and control will shape the implementation of the SAS. The user interface, which is intimately connected to process direction, shapes how the operator views the SAS.

3. Interprocess Communication and Control

A necessary item in the implementation of finely grained processes is the existence of efficient interprocess communication. We see the need for two types of interprocess communication: imperatives, which transfer commands and state information between the processes; and sets of data which are shared among the processes (see Fig. 1-1).

4. Imperatives

Imperatives are the means by which a process directs another process to perform a specific task. They are also the means by which information is carried from one particular process to another. Imperatives are messages from one process directed to a specific other process; or perhaps, from one functional unit to another, where the specific process is defined at another level – the user interface, for example.

These messages do not invoke processes on their own. But, one could use a mechanism by which a message to the process control module could start up a process and then forward a portion of the message to the new process.

Our thinking now is that these messages are relatively short. When large amounts of data are to be passed, the data sets will be used, with the messages giving information about them.

In addition to the normal read and write routines needed to implement this message capability, we also need a check mechanism (which may be combined with the read) to see if a message is waiting to be read. This is different from the usual UNIX method of (when reading) waiting until there is a message to be read, reading it, and then returning control back to the procedure which instituted the read.

5. Named Data Sets

Named data sets are sets of data which are shared among the various processes. They are global "common" areas which are administered by a process dedicated to their administration and well being. Since they are similar to common areas, they must be carefully used to avoid problems.

Any process may create, or destroy, a named data set. All processes which know the name, may access and change the data within the named data set. The names are assigned at creation time, and passed around either by means of imperatives, or as data within other named data sets.

There will be three types of named data sets, each with a different protocol. Named streams are FIFO data paths, similar to UNIX pipes. They would be faster than pipes, and allow a process to have a multiplicity of open pipes. A routine may be needed to check if the stream has any data in it.

Named parametric data sets are similar to the Mod 1 data-access routines. They would be record oriented and carry information about their record structure. They would have the same advantages of upward compatibility as do the Mod 1 data-access routines.

Named waveforms would be the waveform transfer and storage mechanism. A named waveform would contain a single waveform segment, along with a header describing the waveform structure – the data structure, e.g., number of points, not the seismic structure.

These named data sets would be kept in memory. One method of implementing them is to force each of them to have contiguous memory locations, and to reserve one mapping register for access to the current named data set. We could have a low-priority process which would do memory housekeeping when the operator pauses. A reaper would have to be implemented, as well as a method of backing least recently used data sets off onto disk and then back into memory when again required. This would require some knowledge of which modules are using which data sets.

6. The Monitor

A central feature of the SAS organization is the Monitor module. The Monitor has two major responsibilities:

> It dynamically configures the software of the system at the operator's and designers' commands. The Monitor is the method of implementing the idea that multiple processes for performing the same task may exist, and that the actual decision of which process to invoke should be left until the last moment. The operator can control the assignment of processes to functionality, with the full range of features provided by the UNIX shell assisting him in making functional groups from fine-grained processes.
>
> It also serves as a teletype handler, with all keyboard data flowing through it. Commands are interpreted by the Monitor and then passed on to the appropriate process.

The Monitor's communication with the other SAS processes will be implemented with the multiplexed I/O capability provided by Version 7 UNIX. Basically, a multiplexed I/O file is a means by which several data streams can be merged to appear as one. From the multiplexed side, each message sent or received from the file will have a channel identification associated with it; from the other side, each channel will look like a normal file. Once such a multiplexed file is established, messages may be sent in either direction.

Whenever the Monitor is started (at the beginning of a user session), it will set up a multiplexed file with three channels for each process:

> The control channel will be used to receive commands typed in on the teletype and information from the sub-processes.
>
> The standard input channel will be used to pass typed-in commands to the sub-processes.
>
> The standard output channel will be used to collect output messages from the monitor and the sub-processes and pass them on to the teletype.

Whenever a line is typed into the teletype, the Monitor will read it and determine whether the line is a command to the Monitor or one of the running sub-processes by comparing it with lists it maintains. If the command is not found in the command lists, it is assumed to be a shell command line, and the Monitor will invoke the shell and pass it the line for parsing (first setting up the standard I/O channels as described). In this way, all the features of the shell, including redirection of input and output, will be available under the SAS Monitor.

When any SAS sub-process starts up, it is required to perform several housekeeping functions that will provide the Monitor with necessary information about the sub-process. The coder of the sub-process will view this linkage as a series of simple subroutine calls.

Some work has been done on a prototype Monitor to demonstrate the feasibility of these ideas, but problems were encountered with multiplexed I/O software which is a recent addition to UNIX. Comparing notes with others at a UNIX user's group meeting, we found that many installations have had trouble with this software. Various people were working on solutions. Therefore, we decided to suspend work on the prototype Monitor and to concentrate on Mod 2. We assume that, by the time we are ready to turn back to the Monitor, we will be able to profit from what other UNIX users have learned.

R. S. Blumberg
L. J. Turek

C. MOD 1: A PROTOTYPE SAS SYSTEM FOR ALPHANUMERIC DATA

Mod 1 is our first prototype for the SAS: a system that deals only with parametric data in the form of arrival lists and event lists. It was described in detail in our last SATS.[1] Once Mod 1 was operational, we felt that we should lose no time in going on to other stages of the system. Therefore, we decided that the only further work done on the Mod 1 system would be on components that would be carried over into later systems, or any changes that were absolutely necessary for Mod 1 to be usable. Under these guidelines, some minor bugs were fixed and substantial improvements were made to the parameter database access routines described in the last SATS.

In writing software for Mod 1, it had become clear that the logical functions provided by the access routines were entirely appropriate for the types of programs being written, and we decided that these routines should be carried on for use in the final SAS. Therefore, a significant effort was made to make them more efficient, with a resulting speedup of approximately 30 percent and a reduction in size of approximately 25 percent from the initial version.

Even with this improvement, some of the Mod 1 programs are still rather slow, but we feel that this can be attributed to the limitations of the physical environment in which Mod 1 must operate – a multi-user UNIX system running on a relatively slow computer. With the eventual conversion to the SAS configuration – a single-user system on a larger computer – and with some additional indexing features yet to be added to the access routines, we feel that response times will be reduced to acceptable levels.

In spite of its current deficiencies, Mod 1 is a fully operating system which has been used as a working environment for the testing and improvement of such seismic programs as the automatic association and location algorithms.

1. Software Database

One area in which we hoped to gain experience during the Mod 1 project was the management of a diverse software collection undergoing progressive improvement by a number of people.

Since the software was to be developed in stages and the specifications were to change with experience, it was necessary to release, at appropriate points, a consistent set of software for testing. A formal release procedure was required so that programs would match a stable set of documentation after a certain point. Programmers would generally like to make "just one more small fix or enhancement" before freezing a version of a program. That kind of flux makes coordination between modules and effective testing difficult, if not impossible. The diagram (Fig. I-2) gives a generalized view of the structure of the database which we constructed.

The collection of software which corresponded to a set of documentation prepared in advance was termed a "version" and given a number (e.g., Mod 1.1, Mod 1.2,...). All software for a given version was collected under one branch of a directory tree. Within the version directory, there were three types of subdirectories: one for each subroutine library, one for each program, and one for definition files. Within each subdirectory, along with the sources, we would create a command file called "makefile" which could be run to compile all the sources within the subdirectory. A "makefile" was also present in the version directory and contained commands to run all the subdirectory command files. Thus, it was possible to recompile all sources for the version by running the "makefile" in the version directory.

Our method of doing a release consists of collecting all source codes for an agreed upon stage of the development into one branch of a directory tree structure, recompiling the subroutine packages and the programs, correcting any inconsistencies, making the sources read-only except to the release manager, and linking the binaries to publicly accessible names. Public names for libraries, documentation, and executable binaries carry a ".version_number" suffix so that any version of a particular library, program, or document can be obtained. In addition, the currently released version of each item is available under its name with no version suffix. Following the release of a version, all subsequent software changes are then incorporated in the next numbered version, with the exception of serious bugs that make it impossible to test certain features of the release. In the case of such a bug, the person in charge of the release supervises the change and recompiles all related software to insure consistency. It is unrealistic to expect individual software authors to check their own software for consistency on a fixed schedule or to release the software they have developed in time for a release date. One individual must be responsible for a given software release and must insure that binaries for a given version match their corresponding sources.

In doing a release, we have found it necessary to archive within the directory branch for that version, all subroutine libraries and relevant files containing definitions used by the programs. Should these be changed for a later version, it would be impossible to recompile the original sources (for example, in the event of a destroyed binary) without restoring old files. We also found it important to reference such subroutines and files in such a way that no version numbers were mentioned in the sources. This removes the necessity of changing references in source files when copying them to the directory for the next version. In our archiving scheme, the directory structure for a given version was a subset of the structure of subsequent versions.

In general, we have learned that it is important: (a) to collect all files for a particular stage of a project under one directory and its subdirectories, and to make that collection as complete as possible so that outside changes will not destroy the consistency of the software within the branch, even though this implies duplication of files in successive versions; (b) to automate the compilation procedure so that it can easily be duplicated exactly at a later date; (c) to keep files as close as possible to the directory level of other files that depend on them; and (d) to avoid multiple copies of files within a version, although multiple names for the same file can be helpful.

2. Location Routine

The Mod 1 location program uses a modified version of the location program written by Julian.[2] A "C" main program written by Leslie Turek provides the interface with the rest of the Mod 1 package. The basic approach of the location program remains intact, in that a system of linear equations is developed and solved iteratively by a least-squares method for correction vectors. Modifications are as follows:

Previously, the program would weight each arrival's effect according to its standard deviation and residual. This part of the weighting scheme gave us no trouble. Unfortunately, since this program is to be fed initial locations that are potentially poor, weighting by residual (especially during the first few iterations) had disastrous results. We found that good arrivals would be thrown out, often permanently. Presently, weighting is dependent solely on the standard deviation of the arrival, which is set according to what type of phase it is; that is, typically impulsive arrivals are assumed to have been picked more accurately than typically emergent arrivals.

Previously, we could not process events with less than 4 arrivals, as this would result in less than 0 degrees of freedom. Presently, if a 3-arrival event is passed to the routine, it will fix the depth at its present value or 33 km, whichever is greater, and proceed.

Previously, the program applied a damping factor to the correction vectors independent of the number of arrivals. Presently, the damping factor is dependent on the number of arrivals, and if there are more than 20 arrivals the corrections are applied full strength.

Previously, if the routine found that the number of degrees of freedom was less than zero, the location process was halted. Presently, one of two things may happen. If the number of degrees of freedom is equal to -1, then the depth is fixed; if it is less than -1, then the window within which a residual must fall in order for that arrival to be considered usable is increased.

Presently, if the program has used all its allowed iterations and it still has not converged on a final location, then the depth is fixed and another attempt is made to get a stable location.

In order to better simulate the Earth, we have added ellipticity corrections to our travel-time calculations.

The routine has been translated into RATFOR, which will aid any further attempts at modification.

L. J. Turek
D. A. Bach
P. T. Crames
M. A. Tiberio

D. MOD 2: A PROTOTYPE SAS SYSTEM FOR WAVEFORM DATA

Mod 2 is going to be our second major milestone in the effort to implement a complete SAS. Its purposes are to provide experience with the Megatek display hardware, provide a test bed for display software, and provide a test bed for an experimental local waveform database. Although it will use much of the parametric software written for Mod 1, it will not, at least in the early stages, interact in a meaningful way with the Mod 1 database.

Work has been progressing along many fronts, all of which will culminate in a waveform display program, wdsp. Among the sub-projects undertaken and detailed below were: conversion to our system of graphics routines obtained from Purdue University's graphics project; conversion of graphics routines used at our installation for a Tektronix storage display to the

Megatek graphics system; and the writing of experimental programs to explore various features of the Megatek which we will need for the waveform display program. In addition, the basic designs of the waveform display program and the waveform database have been specified. In all, progress is being made in the three areas of Mod 2: understanding the capabilities and finding the limitations of the graphics display hardware, generating useful display software, and designing a prototype local waveform database.

1. Megatek Graphics Terminal

We recently purchased a Megatek 7000 display terminal to be used as part of the SAS. The Megatek is a high-speed vector refresh display terminal, with hardware implemented rotating, scaling, and translating of graphics segments. The refresh capability will be an important feature, since we will be able to move and scale waveforms without erasing the screen, which was necessary on the Tektronix 4014 terminal.

We have also obtained a Data Tablet and a Joystick to be used in conjunction with the display terminal. The Data Tablet is a panel approximately 1-ft^2, with a "pen" which is used to identify a location on the tablet. Megatek software can read the tablet and translate the position of the pen on the tablet into a position on the screen. Hence, we can have a user move the pen and simultaneously track its position with a cursor on the display screen, or move a waveform on the screen corresponding to where he moves the pen.

There is also a switch incorporated in the pen which is activated by pressing the pen down on the tablet. This switch will be useful, since we can track the pen with a cursor until the user presses down activating the switch. When the switch is closed, we can perform some function such as identifying a menu item on the display terminal, or identifying a peak or trough on a waveform.

The Joystick is a spring-loaded stick, normally in the upright position, mounted in a small box. When the user moves the stick, Megatek software can detect the angle of the stick and the distance of the stick from the center position. On the top of the Joystick is a switch button which can be pressed. Since the Joystick has features similar to the Data Tablet, it can be used in a similar manner. In the future, we plan to acquire a Function Switches and Control Dials module (FSCD). The FSCD is a general-purpose device with eight rotatable knobs and sixteen switches with lights. This device, under software control, will be used to move waveforms within a fixed window, to identify points on a waveform, and for general-purpose communication between the user and the software.

2. Purdue Routines

When we acquired the Megatek 7000, we also obtained a library of graphics subroutines written for the Megatek from Purdue University. Included in the Purdue routines are functions to plot lines, move cursors and segments, read the Data Tablet and Joystick, and display text strings. These routines are written entirely in "C". The Purdue routines allowed us to immediately test the Megatek, and to develop several demonstration programs. These routines were also used to convert Graphpac, a set of graphics routines developed for the Tektronix 4014, to run on the Megatek. Besides supplying graphics routines, Purdue University also sent us a device driver for the Metatek. We modified it to conform with our hardware and version of UNIX, and then installed the graphics routines.

3. Graphpac Conversion to Megatek

About one year ago, we developed a set of subroutines and functions to perform graphics on the Tektronix 4014 graphics terminal, called Graphpac. These routines were described briefly in the previous SATS.[1] Since they were written, several seismologists as well as computer personnel have used Graphpac to build displays containing axes, waveforms, and text. With many programs running with Graphpac on the Tektronix, we thought it would be useful to convert Graphpac so that it could be used on the Megatek. An advantage of having Graphpac on the Megatek is that Graphpac routines can be called from Fortran (as well as "C"), which is the language many seismologists prefer to use. Because there are only a few routines in Graphpac which actually output data to the Tektronix, the conversion went smoothly. The Purdue graphics routines for the Megatek were used as an interface between Graphpac and the Megatek 7000. During the conversion, there were several obstacles which we overcame; these included different screen sizes between the Tektronix and the Megatek, different methods of addressing the screen, and simulating the Tektronix crosshairs with the Megatek Data Tablet. All software which runs with Graphpac on the Tektronix can now be run on the Megatek simply by recompiling the program with the converted routines.

4. Initial Experiments with the Megatek Graphics Terminal

A number of programs were written to test various aspects of the Megatek display hardware, and its interreaction with the DEC PDP-11 and the UNIX operating system. Among the programs written was one to scroll sine waves at a speed and direction determined by the Joystick.

This was a very useful program. It revealed two problems at an early stage which we will have to deal with. First, and most easily disposed of, was that the Joystick does not transmit a fine enough indication of its position. This can be solved in two ways: first, by replacing the Joystick with a more sensitive one, or by using a different control method, e.g., a knob. We expect to interface a knob control to the system at an early stage.

The second problem is not as easy to resolve. We found that the UNIX operating system, even when supporting a single user, was not consistent enough to present a pleasing moving display. The rate of movement was too variable for an operator's comfort. To use it as it stands would result in a decrease in operator productivity.

The crux of the problem is that the display computer must be updated in a very consistent manner to support waveform scrolling. Were it not for the scrolling requirement, the existing software would be more than adequate.

There are a number of methods by which we believe we can solve this problem. We can write a "smart display driver" which, from within the kernel, controls waveform scrolling. We can use the TUNE kernel which is being written for the waveform database subsystem. Or, we can use another operating system which is more amenable to real-time programming.

The last option, a change in the operating system, seems the least attractive. It would require a high overhead to support an operating system which would be unique within the Applied Seismology Group. Also, the available operating systems are not as supportive of program development as is the the UNIX operating system which we are now using.

The best option seems to be to use TUNE with co-supervisors of UNIX and a special graphics mini-supervisor. TUNE would handle the communication between them as well as providing the real-time primitives which are required. This would fit into our plans, as we had expected to use TUNE at a later date for efficient interprocess communication.

Since TUNE with a UNIX supervisor is not yet ready, we have implemented a "semi-intelligent" graphics driver as a temporary measure. This graphics unit driver can queue requests to change the display list, and will transmit one for each sync signal received from the graphics display unit. Each change request consists of a block of changes, at different places within the display list. The sync signal is transmitted by the graphics display unit after it completes each scan of the display list. The driver then changes the display list between the time the scan ends, and the next one begins. Thus real-time waveform scrolling can be implemented as synchronized changes to the display list.

Also implemented is a command to clear the queue. This is necessary to stop or change the speed of the waveform scrolling in a timely fashion. This graphics unit driver will probably enable us to produce a Mod 2 waveform display program which will be responsive and reasonably pleasant to use.

5. The Waveform Display Program

The culmination of Mod 2 will be a working waveform display program. This program will display up to twelve waveforms on a screen which has been divided into a number of horizontal bands. This program is not meant to be used, at least initially, for seismic analysis. The commands of the program have been specified, the design process is now proceeding, and some of the service routines have been written.

The commands consist of one or more waveform numbers, a command letter, and a variable number of arguments. A command syntax analysis routine has been written and tested which reads the command from the standard input device, analyzes it, and constructs a structure which contains the information. It also does error checking and only allows valid commands.

Among the commands to be implemented are:

- d Display a named waveform.
- m Horizontally move a waveform, or group of waveforms, to a specific time, or relative to the present time.
- o Overlay two waveforms.
- s Horizontally scroll a waveform or a group of waveforms.
- k Mark a waveform; i.e., attach a marker to the waveform data. This marker contains an ASCII string to identify it.
- r Rescale.
- e Exit.

This set of commands will enable us to test the concepts of the graphics programming we proposed. It will also give us some early experience with person/machine interfaces. The primitives needed to create this program will be used later to implement the final SAS.

The early design showed that we need a block allocation method for the graphics unit memory. A group of memory management routines to perform this task have been written and tested. They perform in much the same way as the allocation scheme for the UNIX memory allocation of the PDP-11.

6. Graphics Display Unit Language Assembler and Linker

Another requirement which was recognized early in the design process of the waveform display program was a need for an easy method of specifying standard pictures. There is a need for a set of static sketches — static in the sense that the specifications of the picture do not change as opposed to the fact that the picture remains in one position or is even displayed on the screen. These static sketches are analogous to library subroutines. They can be combined with other sub-pictures to give a complete display. Examples of these are the graphics associated with waveform marks and axes.

We have decided to build a Megatek Assembler and Linker. The assembler would accept a simple Megatek assembly language, a symbolic representation of its display list language. The assembler would then analyze this input and produce a file which is the octal representation of the input display list. The linking loader would be a subroutine callable from the waveform display program. It would read the output file of the assembler, load the display lists into Megatek memory, and return to the calling program a table of addresses where the various display lists could be found.

The Graphics Assembler is comprised of five modules:

a lexical analyzer,
a simple parser,
a preliminary assembler,
a runtime assembler, and
a linking loader.

The lexical analyzer tokenizes the assembler source input file, dividing it into meaningful pieces for the parser. The parser performs the actual interpretation of the tokenized assembler source. It issues instructions to the preliminary assembler as to how it should produce a character graphics file.

The runtime assembler reads in these character files and produces binary images with possible external references which the linking loader must resolve. The loader also moves the resulting binary graphics "object" to the graphics device.

The assembler source format is not dependent on fixed columnation; spacing is insignificant except to separate the tokens. It does not matter which columns of the line a particular field occupies. Each source line comprises source for a single instruction and consists of an optional label, an instruction and its arguments, and an optional comment. In general, a single mnemonic assembly language instruction will assemble to any one of a variety of graphics processor machine instructions, depending on what the arguments to the instruction are.

SAMPLE INSTRUCTION SET

VEC	Draws a vector, arguments indicate the end point of the vector.
POINT	Plots a single point on the screen, arguments indicate the position of the point.
JUMP	Proceed to specified set of graphics commands.
JSUB	Execute specified set of graphics commands and then resume processing at this point.

ORIGIN	Set the origin of the display to the point specified.
TEXT	Display the text string argument.
TME	Set the elements of the hardware vector transformation matrix.

7. Local Waveform Database Design

We have developed a design for a local waveform database to reside on the SAS host computer and serve as input to the waveform display program and other seismic processing programs. Each database will be named, so that more than one waveform database can be in existence at a given time. In the final implementation of a data center, a local waveform database will be created when the user initiates a data request from the SAS to the waveform database subsystem. While we are still working with an isolated SAS, we have programs to convert data from the .gi/.g format currently in use on the research UNIX system and will provide programs to read in some types of waveform data directly from magnetic tape.

The waveform database designed for Mod 2 will be analogous to the waveform database currently in use on our research UNIX system, with some modifications to eliminate problems which have been noted in the past. Logically, a waveform database consists of a numbered series of waveform segments, with associated descriptive information, sample markers, and dropout flags.

The description file, which in the old format was a fixed-field alphanumeric file, will now be a parameter file which will allow the use of the parameter file access routines developed under Mod 1. Parameters comprising the waveform description file are:

wfno	int	waveform number
station	char(8)	station code
channel	char(8)	channel code
stime	tim_t	start time of waveform segment
etime	tim_t	end time of waveform segment
spsamp	int	sampling frequency
spsecs	int	samp' samples per 'spsecs' seconds
cal	float	calibration
format	char	code for data format 'l' = 32-bit integer

Each waveform data segment will be a binary file containing a continuous stream of samples in the designated format. Data dropouts (data samples not received) will appear with the value of 0.

Markers are a means by which an operator-assigned name is associated with a particular data sample of a waveform. They can indicate phase onset times, peaks and troughs, or anything else required. Markers can be displayed or can be used as an input to seismic processing programs. In the new waveform database, there will be a separate marker file for each waveform segment. It will be in the form of a parameter file, with only two entries in each record: the name of the marker and the sample number it corresponds to.

The dropout file is a new addition. It will be a parameter file, with each record describing a data dropout or glitch in the associated waveform. Parameters will be the starting and ending sample numbers and a code for the type of problem (data never received, data judged to be bad by analyst, etc.).

For purposes of fast scrolling by the display program, it may be necessary to have an additional type of file which incorporates both the marker and dropout information in a form that can be accessed more rapidly. This may not become a permanent part of the database, but may be created only for use by the display program. We call this file the "bit-string file" because it will simply contain one or two bits to indicate, for each sample in the waveform, whether there is some mention of it in the corresponding marker or dropout file. During fast scrolling, this file can be read along with the new data with minimal head movement, and points of significance can be roughly marked as they flash by. When the scrolling stops, the display program can then take the time to retrieve the detailed information from the marker and dropout files and to display it fully.

At our current stage, we need very little special-purpose software to work with these waveform databases. Most of the files can be read and written using either the parameter access routines or regular binary reads and writes. We plan to provide some simple tools, such as a reference file containing structure definitions for the various file types, subroutines to convert from sample times to sample numbers and back, and some simple subroutines to create and unpack the bit-string files.

If this waveform database format proves adequate for our needs in Mod 2, we will then design a higher-level software interface oriented toward the needs of the seismic researcher. Such an interface would include the concept of a waveform segment (with all its associated information) as a data object that can be displayed and manipulated.

R. S. Blumberg
L. J. Turek
M. K. Nahabedian
P. T. Crames

E. DATABASE SUBSYSTEM: DESIGN OF THE TUNE KERNEL

Development efforts on the waveform database have focused on the design and implementation of the TUNE kernel. Presented below is a series of highlights of the kernel design together with information regarding the current state of the implementation.

1. Goals

The major goal of TUNE is to provide a network environment on a single-processor system. Within this environment, sets of processes may operate as individual isolated host units just as they would on their own host. Different types of applications should be provided proper support so that each may be written in such a fashion that it may be transferred to its own host with minimal change. The emulation environment should provide the ability to test systems under various host and network failure scenarios, and also provide a performance testing capability under a wide variety of configuration assumptions.

2. General Structure

The kernel provides to each supervisor a virtual machine similar to, but not identical with, a PDP-11. The differences arise both from idiosyncrasies within the PDP-11 architecture and from efforts to provide a more felicitous interface to the supervisor with the goal of eliminating overhead and supervisor complexity, without eliminating useful flexibility. Reduction of overhead is particularly important, since TUNE is to be used in environments requiring high I/O throughput which cannot be achieved while doing virtual machine simulation of the PDP-11 architecture.

TUNE provides kernel support for multiple-user processes under control of a supervisor. The priorities of these processes and the address spaces associated with them are controlled by the supervisor, this control being exercised by means of explicit calls for kernel services which are made via the EMT instruction. The user tasks may request supervisor services by means of the TRAP instruction, which results in an interrupt fielded by the supervisor.

Besides the EMT instruction, there are two other channels of supervisor-kernel communication. A shared memory area, the supervisor interface area, is mapped into a reserved page of both the supervisor and kernel address spaces and serves as a medium of low-overhead communication. Supervisor interrupts are used by the kernel to notify the supervisor of an external event by diverting the flow of control within a supervisor to a supervisor-specified routine which then may deal with the event.

3. I/O Support

The TUNE kernel provides I/O facilities which aim to remove much of the complexity of interrupt handling and device control from the domain of the supervisor, while retaining as much flexibility as possible for the implementation of diverse supervisors with diverse purposes. Three different types of I/O are distinguished, each handled in a different fashion. The three types are terminal I/O, block I/O, and local network I/O.

The terminal handling code within the kernel is responsible for the handling of character-level interrupts, only interrupting the supervisor when truly necessary. Individual terminal interface modules provide a number of different styles of terminal handling to the supervisors. The supervisors communicate with the terminal interface by setting and interrogating terminal attributes defined by the individual interfaces. The supervisors' communication with the terminal interfaces is mediated by an EMT service routine which provides for the setting and interrogation of several attributes as an indivisible operation.

The block I/O interface provides the supervisor with a simple means of controlling disks and tapes, which isolates the device-specific handling within a kernel driver routine yet provides full support for the asynchronous operations required by the waveform database. Each virtual device owned by a supervisor is represented by a device image located within the supervisor interface area. Space is available within the interface area for the supervisors to construct I/O request blocks which specify I/O operations to be performed. A queue of such request blocks represents the I/O operations to be performed on the virtual device. The supervisor may invoke an I/O operation by placing an I/O request block at an appropriate point within the queue and notifying the kernel of its presence by an EMT instruction. The supervisor is free to choose in what order the I/O operations will be done. When each I/O operation is completed, the next I/O request is taken from the associated queue. The supervisor is notified of the completion an I/O operation by a supervisor interrupt or by waking a specified process.

The interface to the local network, both simulated and real, has not been fully specified. The following considerations will govern the shape of this interface. It should provide the same flexibility and facilities for asynchronism as the block I/O interface. It should provide transparent operation irrespective of whether it is communicating with a supervisor on the same or a different host, while providing very high performance when used between two supervisors on the same host in order to limit the performance penalty which must be absorbed in handling small configurations in this fashion.

4. Virtual Clocks

Both the block I/O and local network interfaces provide for the maintenance of supervisor virtual clocks, which predict the time that the supervisor's execution would require on its own host under the assumptions of the simulation. Virtual clocks are maintained by determining the time that the primitive operations of a given supervisor will take under the given circumstances and using these individual predictions to govern the evolution of the simulation. This requires that interrupts and other items of kernel-supervisor communication be assigned virtual times for their performance. This kernel uses these times to maintain a queue of events to be performed ordered by virtual time, and synchronizes processor access for the given supervisor's processes with these events.

In addition to the intra-supervisor virtual time synchronization required by block I/O, the simulation of local network operations requires inter-supervisor synchronization, to prevent the virtual clocks of the several supervisors from diverging and thereby invalidating the simulation as a whole. TUNE provides for a specifiable window which specifies the maximum permissible divergence among all virtual clocks within a given host.

5. Implementation Status

Considerable code has been written for the TUNE kernel. Some of this has been tested. The tests to date have been rather primitive. Now that the basic facilities of TUNE are working, the test supervisors can assume greater sophistication and test the kernel more rigorously. The following areas have been coded and tested fairly thoroughly: the EMT interface, system initialization, and address space management. The following areas have been coded and have been tested to some degree: process management, virtual clock management, and terminal handling. Two areas remain to be coded: block I/O and local network support. Work on these will proceed once testing of terminal handling and process management is complete.

D. B. Noveck

F. LOCAL COMPUTER NETWORK

The local computer network is needed to interconnect the computers of the Seismic Data Center (SDC) to provide an effective and efficient means of transmitting data and control information between computers. This computer network must serve to interconnect all the computers which will make up the SDC. It must operate very reliably and with a high intercomputer data rate.

The proposals for development of the local computer network were received and evaluated during this report period. Four proposals were received from industry offering several approaches to meeting the requirements of the local computer network. The winning proposal was submitted by Sytek, Inc. A contract for the local computer network was initiated 2 July 1980, and the first design review was held in August. The projected completion of the system is 30 June 1981.

The Sytek plan is to develop a network front-end processor based on a microcomputer. This processor will implement the protocols needed to transfer data between hosts over a 2-Mbps shared cable using CATV (cable access television) technology for data transmission. The data transmission will use the "mid-split" scheme with a standard CATV channel pair – one frequency to transmit, and a related frequency to receive. At the "head-end" (CATV terminology),

a frequency translator will convert all received frequencies up about 150 MHz, and retransmit them on the same cable. The separation of inbound and outbound signals is by standard CATV filters. The mid-split frequency translator is also a standard CATV product. The use of CATV technology allows the extension of the network to the order of kilometers of extent, and the signaling speed to be increased to the order of several tens of megabits per second. The cable TV industry has developed highly reliable amplifiers, frequency translators, cable tapping hardware, etc., which are now readily available for use in data systems. The use of CATV hardware with VHF (very high frequency) modems for local computer networks was pioneered by the MITRE Corporation.[3]

The Sytek approach includes the use of a network front-end processor implemented by Intel 8086 and 8089 chips to perform most of the logic needed to communicate over the network. The 8086 will implement the control of the protocols and the 8089 will control the DMA movement of the data over the Unibus to the front-end memory and from the front-end memory to and from the network transceiver.

The protocols to be implemented include a link level protocol which is a listen-while-talk protocol similar to that implemented by MITRE in their MITRENET system. The key element in this protocol is the transmission of a preamble, and the detection of the correct reception of the preamble for sufficient time to allow all nodes to detect that the system is in use. If a collision is detected, all transmitting hosts stop and wait for a small variable period before trying again.

The next protocol in the hierarchy uses the link protocol and provides the basic transmission of data from one node to another. This is called a transport level protocol and provides unreliable (i.e., no acknowledgments) communication between network front-end processors. This protocol is used by the network front-end processors to implement a reliable datagram protocol, called the transaction protocol, and a reliable stream protocol used to transmit large blocks or streams of data from one host to another.

The host interface is implemented as a set of Unibus registers through which command messages are passed. The command messages are composed in the host memory and the address of the command is passed to the front-end processor. The front end then schedules the operation and interrupts the host when the operation is successfully completed or has failed. The host then can take corrective action for failures, and schedule further operations for successes.

The development of the local network is proceeding on schedule. The delivery of hardware is scheduled for next spring, with a system test period scheduled to end in June 1981 with the completion of the contract.

A. G. Gann

G. SYSTEM DOCUMENTATION: ADAPTATION OF THE "LEARN" PROGRAM

The LEARN program[4] is an interpreter for computer-aided instruction scripts, which is furnished with the Version 7 UNIX system. The program as furnished had several bugs due either to transcription or to changes made locally to our system, mostly the latter. These errors have been corrected and the changes needed to make the scripts correspond with our local system have been completed for the most-used scripts. A new script to familiarize a user with the SDC documentation system[1] has been added.

The LEARN program interprets scripts designed to introduce features of UNIX and to allow users to practice using programs and commands of the system without needing someone to guide and answer questions. The program is furnished with six scripts covering commands and the

UNIX file system (two scripts), the editor, the program for formatting mathematics, the Bell Telephone Laboratories (BTL) documentation formatting routines, and the "C" language. The script on the BTL documentation has been rewritten to apply to the SDC documentation system.

The LEARN program presents the explanatory material from the script on the student's terminal and allows the setting up of files, special commands, and the collection of the student's input and/or output. The student is posed a problem which may require some commands to be used or may require a specific output be generated. Other problems require the answer to a question of the nature "answer N," where N is a number dependent on the question posed in the script. Other script questions require yes or no answers. Depending on the answer, the score is incremented or decremented (between zero and ten) and the next lesson is selected based on the student's current score; then the lessons can be structured in a tree with multiple "tracks," depending on the student's performance.

With the prospect of a wider community of users of our system in the future, the LEARN program provides a valuable capability for a new user to become familiar with the use of the UNIX system without needing a tutor to "hand-hold" the new user. Further additions and corrections of any remaining problems in the scripts will be undertaken as time permits. Comments from users are solicited to help resolve any remaining problems.

A. G. Gann

REFERENCES

1. Seismic Discrimination SATS, Lincoln Laboratory, M. I. T. (31 March 1980), DTIC AD-A091107.
2. Ibid. (30 June 1973), DDC AD-766559/9.
3. G. Hopkins, "Multinode Communications on the MITRENET," Proceedings of the LACN Symposium, Boston, May 1979.
4. B. Kernighan and M. Lesk, "LEARN – Computer-Aided Instruction on UNIX" (Second Edition), UNIX Programmer's Manual, Seventh Edition, Volume 2, Section 7, Bell Telephone Laboratories, Murray Hill, New Jersey (January 1979).

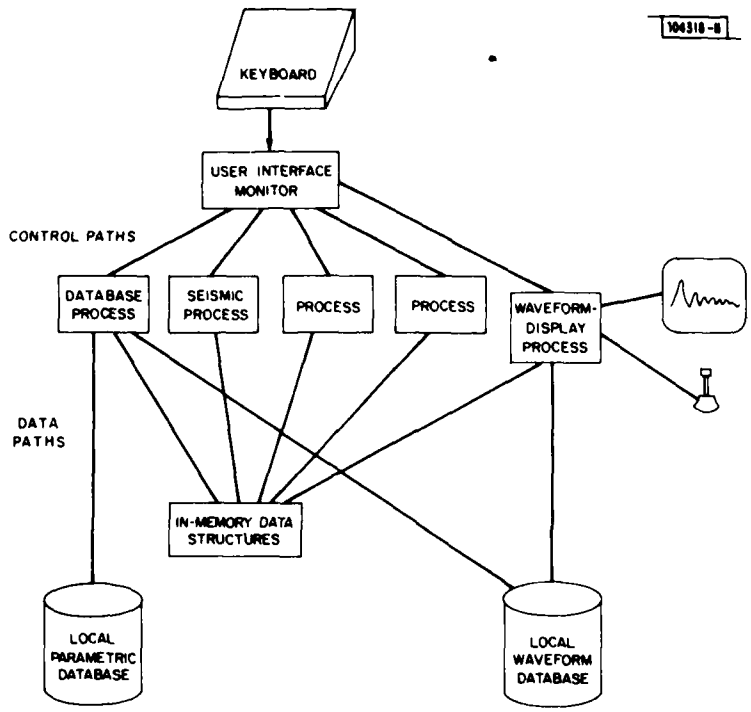

Fig. I-1. Seismic Analysis Station software structure.

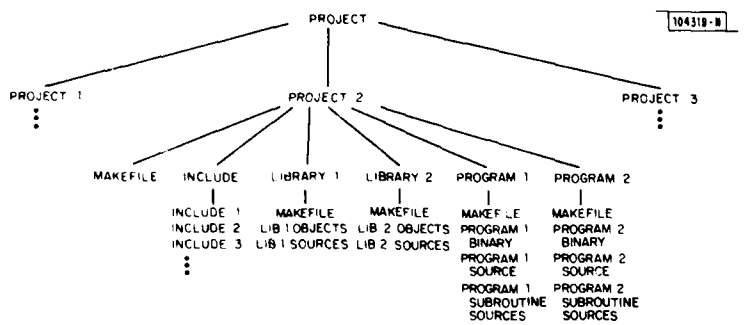

Fig. I-2. Mod 1 software database scheme.

II. SEISMIC ALGORITHMS

A. IDENTIFICATION OF LOCAL EVENTS IN AUTOMATIC SIGNAL DETECTIONS

Of the 17 currently installed SRO/ASRO stations, all but 5 are in regions of moderate to high seismic activity. It is thus inevitable that a large proportion of the signals triggering the automatic short-period (SP) event detector will be from local or regional events. The signals from sources at such distances are of much higher frequency than teleseisms but possess sufficient energy in the 0.5- to 2-Hz band used for detection to trigger the SRO detector. In an earlier SATS[1] it was estimated that over 50 percent of the detections made at the Albuquerque SRO appeared, from their high frequency content, to result from events at distances of probably less than 10°. In the absence of any complete local bulletin for the Western U.S. (events being located on a state basis, with varying levels of effort), this could not be verified.

In Japan, an extensive seismic network is operated by the Japan Meteorological Agency (JMA) which prepares a seismological Bulletin covering Hokkaido, Honshu, and Shikoku, with less complete coverage for Kyushu and the closer islands of the Ryukyu, Bonin, and Kurile chains. For the time interval 10-21 August 1978, we have used both the PDE and JMA Bulletins to attempt to identify the detections made at Matsushiro ASRO (MAJO). We have found that the frequency content of the detection can be used to determine, with a fair degree of success, which signals are from events at distances of less than 500 km. This ability to flag detections as being from close sources can be of extreme value in an automatic association scheme: large signals can be used to provide an initial location, and smaller ones can reasonably be assumed to be from events which will not be detectable at other stations of a sparse global network.

Figure II-1 shows the distribution with magnitude of the events given in the JMA and PDE Bulletins, the shaded portions indicating detection at MAJO. An additional 60 events, mostly in the Western U.S. and not assigned a magnitude, were reported in the PDE; none were detected at MAJO. On the basis of such a small sample, little can be said about the magnitude thresholds of either catalog or the detection capability of MAJO. In the preceding SATS,[2] a 50-percent detection threshold of m_b 5.0 was obtained for MAJO. This performance could certainly be improved by lowering the detector threshold, but this could only be achieved at the undesirable cost of greatly increasing the number of local events detected. The JMA Bulletin is certainly incomplete, as it shows no increase in the number of events in decreasing magnitude.

Of the 129 detections made at MAJO, 40 could be associated with PDE events at distances of 10° or greater, 34 with JMA events at distances of less than 10°, and 55 were unassociated. Sample signal spectra of local and teleseismic events are shown in Fig. II-2, together with the background-noise level which several independent samples showed to be very stationary. As expected, signals from local events were dominated by high frequencies (2 to 5 Hz), while teleseisms were predominantly lower frequency (0.3 to 2 Hz). In both types there was a very large variation in spectral shapes from event-to-event, which is not encouraging for detector design based upon spectral shape of signal and noise. There was some indication that some of the local signals were perilously close to, if not actually, aliased.

We have attempted to discriminate between local and teleseismic signals on the basis of their frequency content. Both frequency- and time-domain measurements were attempted, as was the dominant period at peak signal amplitude. The most successful of these was the ratio of the powers $\Sigma\, s_f(t)^2$ in the signal s(t) after bandpass filtering into high- and low-frequency

TABLE II-1
NETWORK III

Station Code	Latitude	Longitude	Noise Level	Travel-Time Anomaly	m_b Bias	Location
afi	-13.91	-171.78	40.00	0.21	-0.10*	New Zealand
ale	82.48	-62.40	5.00	-0.58	-0.04	Canada
anmo	34.95	-106.46	2.00	0.19	-0.20	United States
anta	39.90	32.78	2.00	0.10	0.10*	Turkey
are	-16.46	-71.49	7.00	-0.23	-0.10*	Peru
asp	-23.68	133.90	3.00	-0.75	-0.05	Australia
BDF	-15.66	-47.90	3.00	-0.36	0.10*	Brazil
bng	4.44	18.55	1.00	-1.25	-0.07	Central African Republic
boco	4.59	-74.04	2.00	1.21	0.04*	Columbia
bod	57.85	114.18	5.00	-0.85	0.10*	USSR
bul	-20.14	28.61	4.00	-0.72	-0.07	Rhodesia
chto	18.79	98.98	2.00	-0.65	0.00*	Thailand
col	64.90	-147.79	5.00	-0.51	0.01	United States
com	16.25	-92.13	25.00	0.79	0.00*	Mexico
dag	76.77	-18.77	12.00	-0.59	-0.02	Denmark
EKA	55.33	-3.16	8.00	0.12	0.19	United Kingdom
elt	53.25	86.27	5.00	-0.72	0.10*	USSR
goco	45.70	-75.48	2.00	-0.21	0.10*	Canada
GBA	13.60	77.44	15.00	-0.16	0.04	India
GRF	49.69	11.21	2.00	0.18	0.24	Federal Republic of Germany
HFS	60.13	13.70	1.00	-0.51	0.05	Sweden
ifr	33.52	-5.13	8.00	0.32	0.00*	Morocco
JYSA	62.17	24.87	2.00	0.00*	0.20*	Finland
khc	49.13	13.58	3.00	-0.32	0.10	Czechoslovakia
kic	6.36	-4.74	3.00	-0.85	-0.05*	Ivory Coast
KSRS	38.00	128.00	3.00	0.00*	0.10*	South Korea
LAO	46.68	-106.22	0.40	-0.11	-0.10	United States
maio	36.31	59.49	2.00	0.90	0.00*	Iran
mat	36.54	138.21	10.00	-0.54	0.00*	Japan
maw	-67.60	62.88	10.00	-0.11	0.11	Australia
mbc	76.24	-119.36	6.00	-0.41	0.14	Canada
NAO	60.82	10.83	0.80	-0.75	-0.09	Norway
nie	49.42	20.32	5.00	0.28	-0.02	Poland
niko	-1.27	36.80	2.00	1.56	-0.20*	Kenya
obn	55.12	36.57	6.00	-0.47	0.20*	USSR
pns	-16.27	-68.47	3.00	0.24	-0.08	Bolivia
que	30.18	66.95	10.00	0.25	0.10*	Pakistan
sba	-77.85	166.76	30.00	0.69	0.10*	New Zealand
shio	25.57	91.88	2.00	-0.54	0.11	India
sna	-70.32	-2.33	16.00	-0.13	-0.05*	South Africa
spa	-90.00	0.00	8.00	0.02	0.10*	United States
sve	56.80	60.63	6.00	-0.18	0.20*	USSR
tam	22.79	5.52	4.00	-0.19	0.00*	Algeria
tato	24.98	121.49	4.00	0.00*	0.00*	Taiwan
tll	-30.17	-70.80	12.00	-0.30	-0.10*	Chile
wel	-41.29	174.78	30.00	-0.31	-0.10*	New Zealand
wes	42.38	-71.32	15.00	0.35	0.10*	United States
WRA	-19.95	134.35	2.00	-1.06	0.00*	Australia
yak	62.02	129.72	5.00	-0.89	0.10*	USSR
YKA	62.49	-114.60	3.00	-0.76	-0.07	Canada

* Estimated using neighboring stations.

bands. The apparently equivalent frequency-domain analog (spectral ratios) was less successful probably due to windowing and truncation effects.

Optimum distance discrimination was found to be realized by the ratio of signal power in the 3- to 8-Hz band to that in the 0.3- to 1-Hz band. The ASRO instrument response peaks at about 2.5 Hz and falls off rapidly below 0.5 Hz and above 6 Hz, so this is very close to the ratio of power at 3 Hz to that at 1 Hz. Figure II-3 shows this ratio as a function of distance Δ. It can be seen that all associated signals with a ratio greater than 0.1 are at distances of 5° or less, and that all those with a ratio less than 0.03 are more than 10° distant from MAJO. Between these two values there is a "gray" area.

In Fig. II-3, events at depths of less than 70 km are designated by S, and those at greater depths by D. A presumed explosion in Novaya Zemlya is denoted by X. The intrinsically higher-frequency nature of teleseisms from deep events can be seen. At closer distances, one would expect this character to be negated to some extent by the low Q structure beneath Japan; this is not apparent. While the distance discriminant probably works because of the higher attenuation at high frequencies, seismic scaling effects cannot be discounted since the closer events are mostly much smaller in magnitude than the teleseism. The events at distances of less than 10° which fall into the "gray" area are indeed among the largest at close distances.

Of the 55 unassociated signals, all but 15 had ratios of 0.1 or greater, indicating that they were almost certainly from local events. It appears that local events recorded at MAJO can be readily identified on the basis of their frequency content, and that such identification can certainly be applied to other stations beneath which Q is probably higher than for MAJO. The broader-band response of the NSS instrumentation should make such identification even easier, and we propose to test this as soon as the data and (more importantly) local bulletins become available.

R. G. North
M. W. Shields

B. A TEST OF AUTOMATIC ASSOCIATION ALGORITHMS USING SYNTHETIC DATA

Lists of synthetic arrivals at a global network of stations have been compiled, and used to examine some of the characteristics of automatic and manual methods for event association and location. The lists are generated by first computing a set of synthetic seismic events, realistically distributed in space, time, and magnitude, and then computing arrivals at a prescribed global network of stations using a variety of acceptance criteria which attempt to model scattering in the Earth, regional variations in travel times, station detection capability, and operator error. Details of this procedure have been given earlier.[2]

The network of stations used is the Network III(SP) listed in document CCD/558, issued by the Committee on Disarmament (CD) Group of Experts on 9 March 1978. The stations in this network are listed in Table II-1 which also includes station noise levels (as listed in CCD/558), station travel-time anomalies (Dziewonski[3]), and station amplitude biases.[4] Where travel-time anomalies or amplitude biases were not available, they have been estimated from values at neighboring stations.

Three arrivals lists, each corresponding to one day, were generated for this network, and the principal characteristics of these lists (referred to as A, B, and C) are shown in Table II-2. List A contains only larger events, while list C includes events down to $m_b = 2.1$. It appears that an average day of seismicity will lead to about 1000 arrivals at a network such as the one

TABLE II-2

CHARACTERISTICS OF THE ARRIVALS LISTS

	List A	List B	List C
Period Covered	1 day	1 day	1 day
Event List Complete Down to m_b	4.3	2.7	2.1
Total Number of Events in List	32	862	3802
Number of P Arrivals at Network III	500	840	814
Number of pP Arrivals	93	89	69
Number of S Arrivals	37	60	30
Number of Events with at Least 25 Arrivals	5	7	6
Number of Events with at Least 10 Arrivals	19	26	15
Number of Events with at Least 5 Arrivals	28	41	35
Number of Events with at Least 3 Arrivals	30	59	51
Number of Events with at Least 1 Arrival	30	172	302
Number of Events with 0 Arrivals	2	690	3500
Number of Local Arrivals (<5°)	3	58	182
Number of Non-local Arrivals (>5°)	497	782	632

used here, and this is useful for sizing the task of data analysis for such a network. Natural variations in seismicity may lead to substantial variations from this average, particularly when earthquake swarms or aftershock sequences are present.

The three arrivals lists were each analyzed by two automatic-association algorithms currently in use in the U.S. The first, which we refer to as Procedure 1, utilizes P-wave arrival times and depth-phase arrival times (the latter are not used for association, but are included in the computation of the hypocenter parameters). To define an event, 5 arrivals are required, and array data are not used. The second, Procedure 2, does not use depth-phase information, but does utilize array estimates of azimuth and distance for trial epicenters. In this case, a minimum of 3 arrivals is required to define an event. Event solutions for 3 or 4 arrivals are computed by restraining the depth to zero.

The event lists generated by these algorithms were compared with the original event lists. The quality of the event solution was defined in terms of the accuracy of the epicenter location. If δ is the sum of the absolute values of the errors in latitude and longitude, then the event quality is assigned as follows:

$\delta \leqslant 0.5°$	Good
$0.5° < \delta \leqslant 1.0°$	Fair
$1.0° < \delta \leqslant 10°$	Poor
$\delta > 10°$	Bogus event

The results from Procedure 1 are summarized in Fig. II-4. Detection and event quality are excellent for $m_b \geqslant 4.5$. Below this magnitude, poor solutions and missing events begin to dominate. In this case, 5 bogus events were generated by the algorithm, each with 5 arrivals.

Procedure 2 gave improved results (see Fig. II-5). More events were detected for $m_b < 4.0$, and the quality of solutions in the range 4.0 to 4.5 is improved. A substantial number of missing events is still present, since the original lists contained many events with 3 or 4 arrivals. Using this algorithm, 13 bogus events were generated from groups of 3 or 4 arrivals, and 1 bogus event was formed from 5 arrivals.

In order to compare these automatic procedures with the capability of a human analyst, an experienced analyst was asked to carry out manual association on the same data. At least 3 arrivals were required to define an event. The results are shown in Fig. II-6. The human analyst performance is substantially better than the automatic procedures. Only a small number of events was missing, though misassociations did lead to a number of poor solutions. Three bogus events were obtained – two with 3 arrivals and one with 5 arrivals.

Several conclusions can be made from this study. Automatic procedures are still quite inferior compared with a human analyst. Additional research is needed in an attempt to improve the performance of the automatic algorithms. Also, the choice of criterion for event definition has a large impact on the final event list. Network detection capability is substantially improved when events with 3 or 4 arrivals are included, but this improvement is accompanied by an increase in the number of missing and bogus events. Finally, even an experienced analyst is not perfect and, in practice, there will always be some (hopefully few) bogus events in the final event list.

M. A. Chinnery
M. A. Tiberio

C. A COMPARISON OF RELATIVE AND ABSOLUTE EARTHQUAKE LOCATIONS IN AN ISLAND ARC REGION

Quantifying the effects of laterally heterogeneous Earth structure should be easiest in regions of active subduction where there are many geophysical, geochemical, and geological studies that claim to have observed such effects. Here we compare earthquake epicenters from the Bulletin of the International Seismological Center (ISC) with relative epicenters computed from the same arrival-time data. The relative epicenters are more clustered and show an apparent westward offset of about 12 km.

The relative location scheme has been described earlier.[1,3] In the previous applications of this scheme, relative depth was of as much, if not more, interest than the relative epicenters because any accurate measure of source depth, whether it be relative or absolute depth, has a potential application to the discrimination problem. However, in island arc regions and other regions that are predominantly water covered, an accurate epicenter may be sufficient to identify an event as an earthquake, rather than an underground explosion, if its epicenter is in deep water.

Accurate epicenter determinations in island arc regions require techniques that, to some extent, are transparent to strong lateral variations in crust and upper-mantle structure exemplified by the inclined zones of mantle seismicity. The master earthquake technique used here is expected to be less sensitive to lateral heterogeneity than the standard bulletin location technique, because the location problem is reduced to a near-source problem. Here, the near-source region is defined by a hemisphere of about 100 km radius centered on the master earthquake. To eliminate trade-offs between relative depth and relative origin time and epicenter, the activity is assumed to occur at the depth of the master.

Shallow activity near the southern terminus of the Philippine Trench is well suited for this comparison because of the intensity of shallow activity and the structural complexity which might impart systematic errors to ISC locations. About 200 earthquakes, of which only 5 were reported with a mantle depth, were located relative to the major-size earthquake (M_S 7.8) of 2 December 1972. The source region is shown in Fig. II-7. The ISC and relative epicenters are shown in Figs. II-8 and II-9, respectively. Clearly the relative epicenters are more clustered and, in particular, the clustering reveals at least three aseismic regions surrounded by comparatively intense activity (regions A, B, and C in Fig. II-9). In addition to the clustering, there is an apparent shift of the relative epicenters to the west by about 12 km relative to the ISC epicenters. If this is interpreted as a systematic error in the ISC locations, then the ISC location for the master must be taken as correct. We cannot prove such an assertion but merely point out that the azimuthal coverage for the epicenter determination of the master is as good as can be expected for this region and, consequently, an accurate determination is possible in spite of the structure complexity of the region because the epicenter is determined more on geometric considerations than on structural ones.

T. J. Fitch
R. Catchings

D. SOME SUGGESTIONS FOR IMPROVING THE ACCURACY OF HYPOCENTER DEPTH ESTIMATES

The purpose of this report is to describe some problems encountered in the use of pP and sP for depth determination of shallow focus oceanic earthquakes. Some ways of overcoming these problems are suggested.

TABLE II-3

DATES, LOCATIONS, DEPTHS, AND MAGNITUDES OF EVENTS ANALYZED

Date	Time	Latitude	Longitude	Present Study	ISC	PDE	m_b	M_s
10/23/64	01:56:05.1	19.80	56.11	25	43	31	6.2	6.4
08/19/77	05:08:41.6	−11.15	118.39	18	54	33	6.1	5.4
08/20/77	19:16:32.7	−11.03	119.13	17	33	33	6.0	6.1
08/25/77	18:05:10.8	−10.74	119.26	11	51	33	6.1	6.0
08/26/77	08:26:37.5	−10.66	119.30	14	33	33	5.6	5.7
09/02/77	10:36:28.3	−11.04	119.14	09	74	33	6.0	5.9
09/23/77	05:57:55.6	−11.20	118.21	24	34	33	6.0	5.4
10/07/77	12:10:43.7	−09.96	117.31	14	29	33	5.9	6.3
10/16/77	21:09:17.7	−09.73	117.11	12	39	33	5.6	5.8

SPZ and LPZ WWSSN seismograms of one Atlantic and seven Western Pacific earthquakes provide the database for the analysis. Table II-3 lists source parameters, and compares depths found in this study with those published in the EDR and ISC Bulletins. The analysis, following a procedure described by Forsyth,[6] consists of a search for phase arrivals within 30 s after the P arrival on each in a suite of SPZ seismograms. If the earthquake is of sufficient magnitude ($M_s > 5.5$), the P waveforms on the LPZ seismograms are also examined.

SPZ seismograms from the earthquake of 20 August 1977 are shown in Fig. II-10. In each case, the important phases are marked on the SPZ seismogram of the station named on the left. The seismograms are lined up so that the zero line represents the first arrival on each seismogram. In the simplest case, one would expect to see the predominant phases: the direct P arrival, the P wave reflected from the rock-water interface just above the hypocenter (pP), and the S wave reflected as P from the same area (sP) plus later phase from reverberations in the water layer. Furthermore, the pP-P and sP-P time differences are functions mainly of depth; at crustal depths, these times vary only a few tenths of a second over the distance range from 30° to 90°. Therefore, these phases would nearly line up on a diagram such as Fig. II-10.

Figure II-10 departs from the ideal and thus illustrates several problems in identifying depth phases. First of all, an earthquake is sometimes closely preceded by a much smaller event, called a precursor. Second, pP and sP are often not particularly prominent on SPZ seismograms. Third, water reflections are often mistaken for pP and sP. Finally, the arrival of a later phase may be lost in the coda of an earlier one.

The precursor problem is common enough so that it must always be anticipated. Figure II-10 shows a precursor on several seismograms. It is recognized as such because, over the entire 110° range of azimuths, its amplitude remains much smaller than that of the next succeeding arrival (the direct P arrival of the main shock). Carefully monitoring the relative amplitudes of the early phases should be an aid in identifying these small events. For example, Kanamori and Stewart[7] judge the Gibbs Fracture Zone earthquake of 16 October 1974 to be an 11-km-deep event with a precursor. They identify the precursor on the basis of low-amplitude first arrivals

TABLE II-4

EXPECTED X-P TIMES FOR FOUR PHASES ASSUMING MODELS OF TABLE II-5 AND VERTICAL RAY PATHS

Model	pwP	swP	pwwP	swwP	Earthquake Depth (Below Sea Floor) (km)
Basin	9.4	10.8	15.4	16.8	10
	10.7	12.5	16.7	18.5	15
	12.0	14.2	18.0	20.2	20
Trench	11.5	13.5	18.3	20.1	10
	12.8	15.3	19.4	22.0	15
	14.0	17.0	20.7	23.7	20

TABLE II-5

PARAMETERS OF OCEANIC BASIN AND TRENCH MODELS*

Layer	Thickness (km)		P Velocity (km/s)	S Velocity (km/s)	Density (g/cm^3)
	Basin	Trench			
Water	4.5	5.0	1.5	0.0	1.03
Sediment Layer 1	0.5	2.0	2.0	1.0	1.50
Sediment Layer 2	1.5	3.0	5.0	2.77	2.58
Crust	5.0	6.0	6.4	3.70	2.85
Mantle	–	–	7.9	4.55	3.305

* Table 3 from Ward.[9]

on all seismograms. An 11-km focal depth is reasonable for an earthquake located on a transform fault. The P wave of the main shock follows the precursor by 11 to 12 s and is identified in the ISC Bulletin as pP. Depth is estimated to be 41 km, unreasonably deep for an earthquake on a transform fault.

The last three problems mentioned above are worst for earthquakes with $m_b \cdot 5.5$. The lack of prominence of pP and sP on SPZ seismograms arises from two causes. First, short-period energy is sensitive to finer detail of crustal structure resulting in a greater number of reflections. If $m_b > 5.5$, more energy is available for transmission through and reflection from various crustal layers, increasing the number of phases recorded on the seismogram. Furthermore, if a thick layer of soft sediment lies above the harder crust, the reflection coefficients for pP and sP are much reduced relative to reflections from other layers. The second cause is variation of amplitude due to radiation pattern. The MAT SPZ seismogram of Fig. II-10 illustrates this best. The focal mechanism deduced for this earthquake predicts a pP relative amplitude of nearly 0.0 at MAT, a prediction justified by the insignificant pP phase on the seismogram.

Reflected phases most often confused with pP and sP for shallow oceanic events are reflections from the water-air interface called pwP and swP (Chen and Forsyth[8]). These phases are quite prominent on short-period seismograms, and it was found in Forsyth's and in this study that their misidentification often leads to overestimation of hypocentral depth by factors of 2 or 3 in bulletins. Table II-4 presents expected phase-P times for four water-air reflected phases based on the oceanic basin and trench models of Table II-5 (Ward[9]).

The water-reflection problem combines with the coda problem as the major causes of incorrect focal-depth estimates. On seismograms of large, shallow oceanic shocks, the pP arrival is often obscured by the coda of P. For a 10-km-deep quake, the pP-P time is only 3 s and sP-P is 4.3 s on teleseismic records. If the quake magnitude is large, all three phases and their codas are inseparable and thus are reported as one. The next identifiable phase at 10 s after P is pwP. Taking this to be pP results in a depth estimate of about 33 km, a threefold overestimate. Nearly all the depth discrepancies between this study and the ISC Bulletin can be traced to misidentification of pwP or swP as pP.

The chaotic nature of the SPZ seismogram for a large shallow oceanic earthquake makes it important that the early part of the LPZ WWSSN seismogram be analyzed when available. The impulse response of the LPZ instrument is shown in Fig. II-11. The analysis assumes that for shallow events the LPZ P waveform is the convolution of impulsive P, pP, and sP arrivals. Phases pP and sP can often be identified as points where the waveform departs from the impulse response to a single phase arrival. These two phases are relatively more prominent on the LPZ than the SPZ record because pwP and swP are mainly short-period phases (Forsyth[6]). On LPZ seismograms for relatively deep events (e.g., Fig. II-12, depth 14 to 16 km), a pP or sP arrival will be seen as a shelf-like offset of the early part of the waveform. On LPZ seismograms from a very shallow event (e.g., Fig. II-13, depth < 10 km), the P waveform will be a smooth convolution of three impulses and will not resemble the LPZ WWSSN impulse response. The deduction follows that SPZ arrivals with phase-P times of 10 s or longer are probably water reflections.

For earthquakes with magnitudes less than about $m_b = 5.5$, the P wave signals are too weak to be seen on most LPZ records but the SPZ record is usually easier to analyze. Incorrect focal-depth estimates are most likely to be the result of failure to recognize a precursor or a low-amplitude pP.

Two other phenomena should also be noted as qualitative indicators of shallowness. First, on the LPZ record, a signal pictured in Fig. II-13 and called "ringing P" by Ward[9] is a probable indicator that most of the fault break is in the crust. Like Ward, the amplitude of the ringing P wave we observed did not vary systematically with focal depth. Second, 9- to 12-s period surface waves on SPZ records of earthquakes with moderate magnitudes indicate shallowness.

M. W. Shields

E. NEW APPLICATIONS SOFTWARE

Four pieces of software which recently have been released are described below.

dt: a power detector. Presently, we have no need for a detector; however, in the future we expect that continuous SP data will be fed to the data center and so we have begun testing a detector. Since real-time data are not available, we have used a tape of continuous (predetector) SRO output which has enabled us to optimize our detector, the limitations being that our data files are of finite length. Dt uses a sliding window 1.5 s long over which the power is calculated, compared with the average power statistics for noise taken 13 s prior to the test point, as its basic detection criterion.

When the test power exceeds 3.5 times the standard deviation of the average noise, a detection is declared and the average noise statistics are frozen. In the same fashion as the SRO detector, our program places a marker "START" 15 s before the arrival. The arrival time is then marked by "ARVL." The detection is declared over when the power is below the threshold for at least 10 s, at which point a marker "END" is written. This leaves the important parts of the continuous record labeled for extraction later. A bulletin of arrivals and detector on and off times is printed.

ppick: a specialized version of dt. SRO records presently are received with little indication of where the arrival is in the record. For a researcher or analyst to make the picks can sometimes be a long and tedious task. Ppick is written to be fast; it will search the first 60 s of the SRO record. Ppick gets its noise averages from the first 14 s of the record and does not update with later values. Thus, if there is less than 14 s of noise before the arrival, chances are the arrival will not be picked. An example of ppick's performance is given in Fig. II-14 which shows the P wave arrivals from some selected Eastern Kazakh "events" as recorded by the Albuquerque, New Mexico SRO. The markers without labels are produced by ppick. Ppick makes no attempt to identify the phase. Those markers labeled "J-B" are produced by another piece of software we have. Their position is calculated from the station and event location as well as J-B travel-time tables. The markers labeled "H" were placed there by myself. The superior quality of the detector picks over the J-B calculated picks is clearly evident. The detector has the added bonus that it requires no a priori knowledge of the event.

grmcrs: a graphics program. Grmcrs can display the phase spectrum of the crosscorrelation of two gramfiles. It can also display the amplitude spectrum of the autocorrelation of a gramfile. This program was developed at the request of one of our researchers who was looking for a way to view the source generated phase differences between path equalized seismograms. The program, which works on LP and SP data, was later expanded to its present state.

polypack: an interactive polynomial calculator. Polypack was developed during an instrument response study. Essentially, the user can input up to 20 polynomials of up to 35th degree.

Basic mathematical manipulations such as addition, subtraction, multiplication, division, square root, root finding, and evaluation are available. All math is done in double precision.

M. A. Tiberio

REFERENCES

1. Seismic Discrimination SATS, Lincoln Laboratory, M.I.T. (30 September 1978), DDC AD-A065574/6.
2. Ibid. (31 March 1980), DTIC AD-A091107.
3. Ibid. (31 March 1979), pp. 21-39, DDC AD-A073772/6.
4. R. G. North, "Station Magnitude Bias – Its Determination, Causes, and Effects," Technical Note 1977-24, Lincoln Laboratory, M.I.T. (29 April 1977), DDC AD-A041643/8.
5. W. Hamilton, "Tectonics of the Indonesian Region," Geological Survey Professional Paper 1078, U.S. Government Printing Office, Washington (1979).
6. D. W. Forsyth, "Determinations of Focal Depths of Earthquakes Associated with the Bending of Oceanic Plates at Trenches," to be published in Physics of the Earth and Planetary Interiors.
7. H. Kanamori and G. S. Stewart, "Mode of the Strain Release Along the Gibbs Fracture Zone, Mid-Atlantic Ridge," Phys. Earth Plan. Int. 11, 312-332 (1976).
8. T. Chen and D. W. Forsyth, "A Detailed Study of Two Earthquakes Seaward of the Tonga Trench: Implications for Mechanical Behavior of the Oceanic Lithosphere," J. Geophys. Res. 83, 4995-5003 (1978).
9. S. N. Ward, "Ringing P Waves and Submarine Faulting," J. Geophys. Res. 84, 3057-3062 (1979).

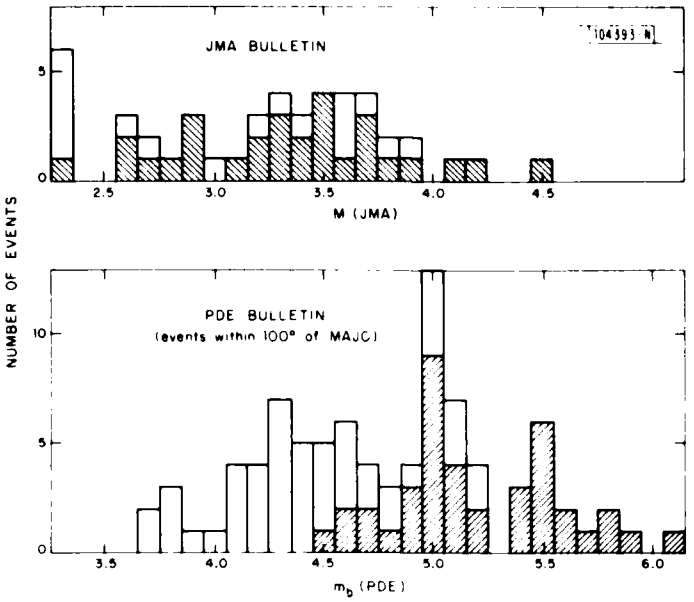

Fig. II-1. Event distribution with magnitude for PDE and JMA Bulletins for 10-20 August 1978. Shaded portion denotes signal detection at MAJO.

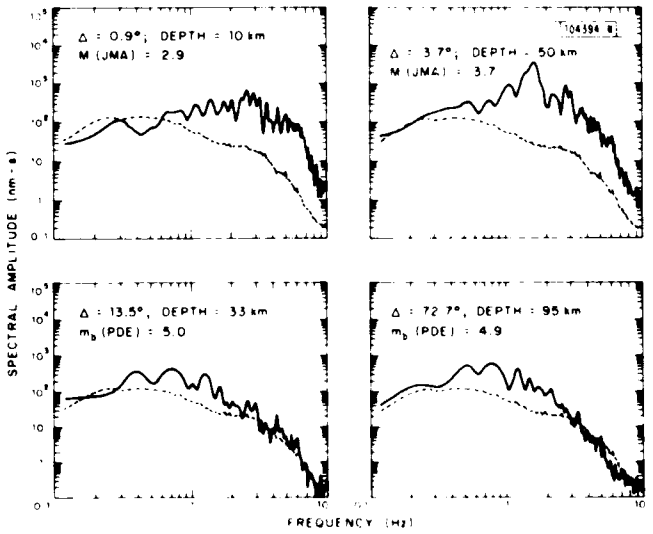

Fig. II-2. Sample signal spectra. RMS noise level shown by dashed line.

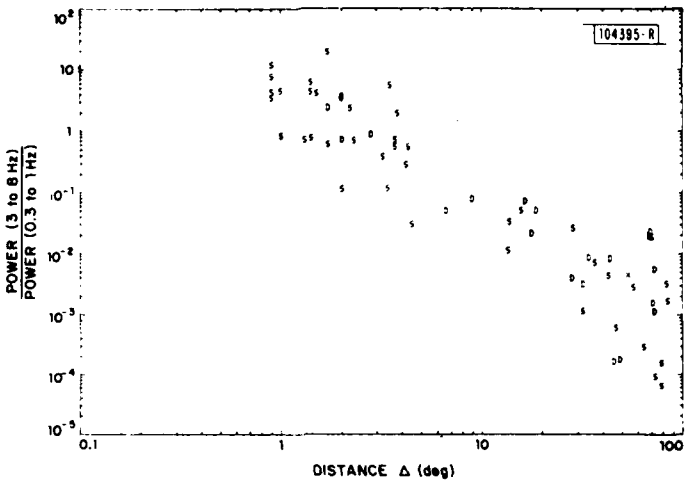

Fig. II-3. Ratio of signal power in 3- to 8-Hz and 0.3- to 1-Hz bands as a function of epicentral distance Δ in degrees.

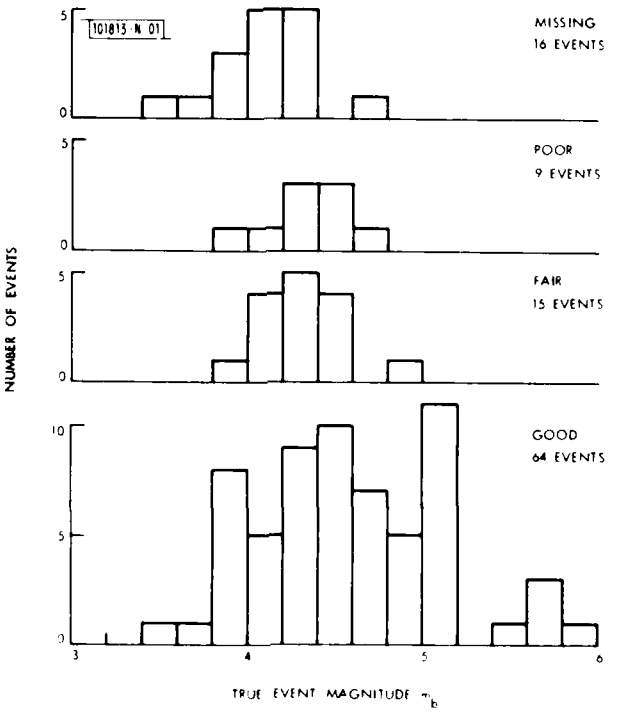

Fig. II-4. Event quality for automatic association as a function of true event magnitude (Procedure 1). Two events with $m_b > 6.0$ are not shown. Counts are summed over lists A, B, and C.

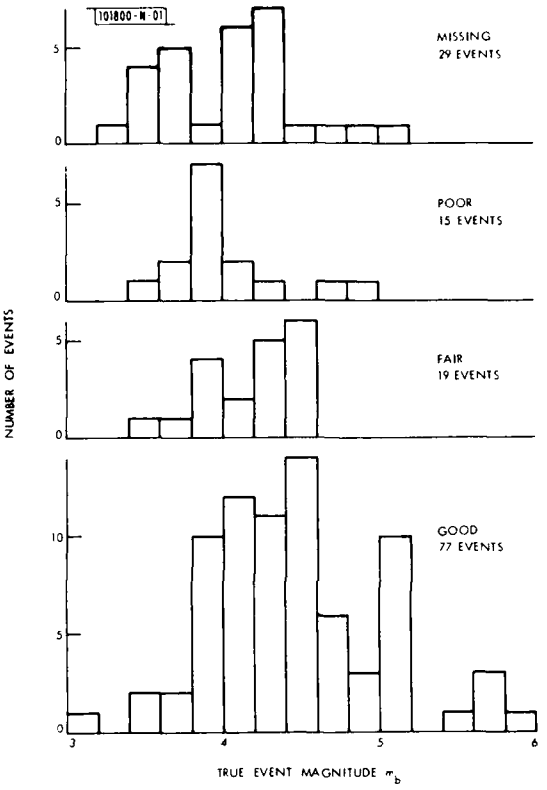

Fig. II-5. Event quality for automatic association as a function of true event magnitude (Procedure 2). Two events with $m_b > 6.0$ are not shown. Counts are summed over lists A, B, and C.

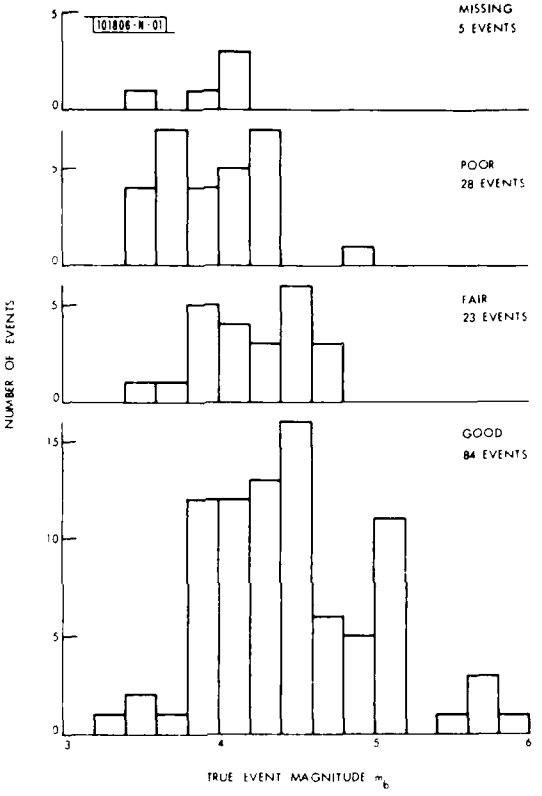

Fig. II-6. Event quality as a function of true event magnitude for manual association by an analyst. Two events with $m_b > 6.0$ are not shown.

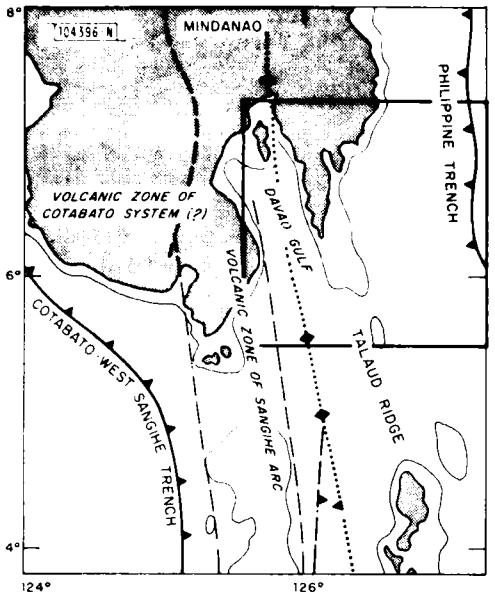

Fig. II-7. Southern Philippine region (from Hamilton[5]).

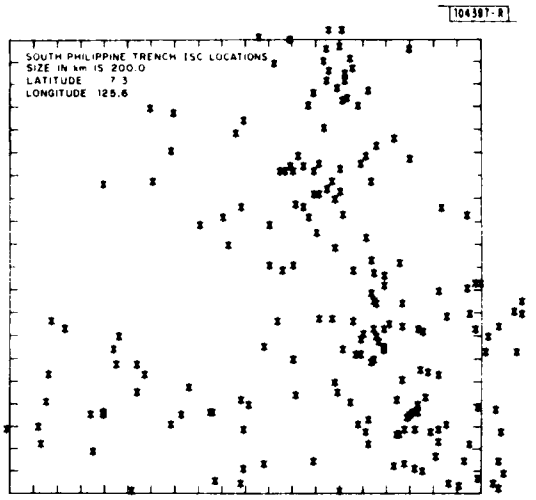

Fig. II-8. ISC epicenters.

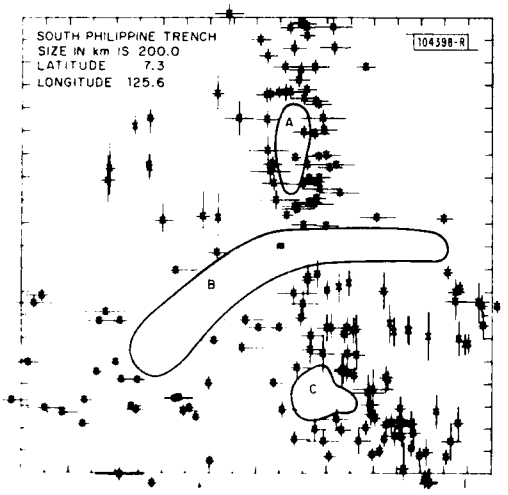

Fig. II-9. Relative epicenters with error bars of one standard deviation.

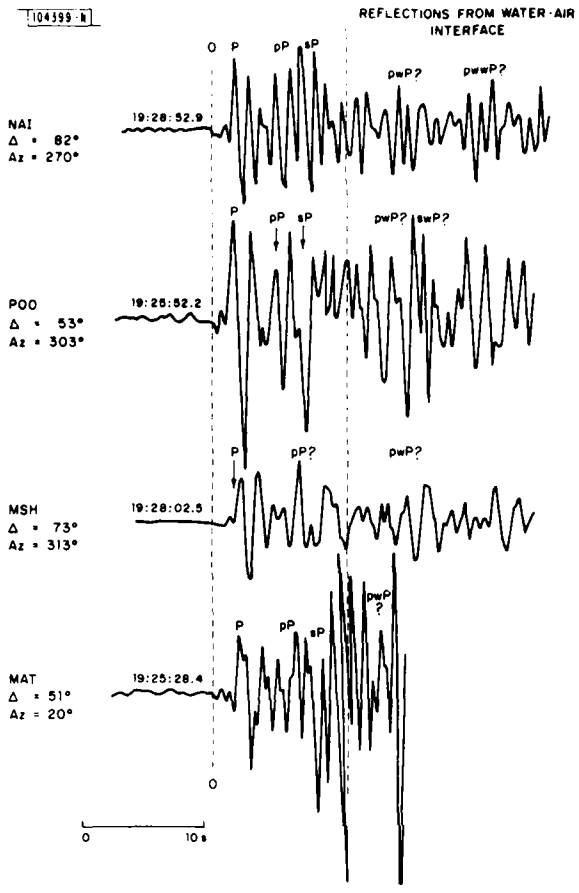

Fig. II-10. SPZ WWSSN seismograms for earthquake of 20 August 1977.

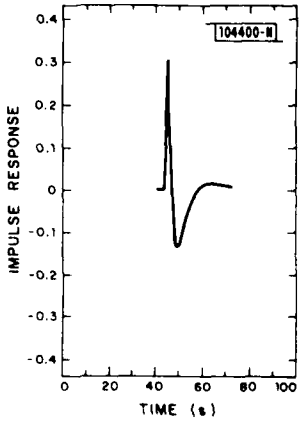

Fig. II-11. Impulse response for WWSSN LP instrument broadened by a t* of 0.5 s. Rise and fall times of impulse = 1.00 s; width = 0.00 s.

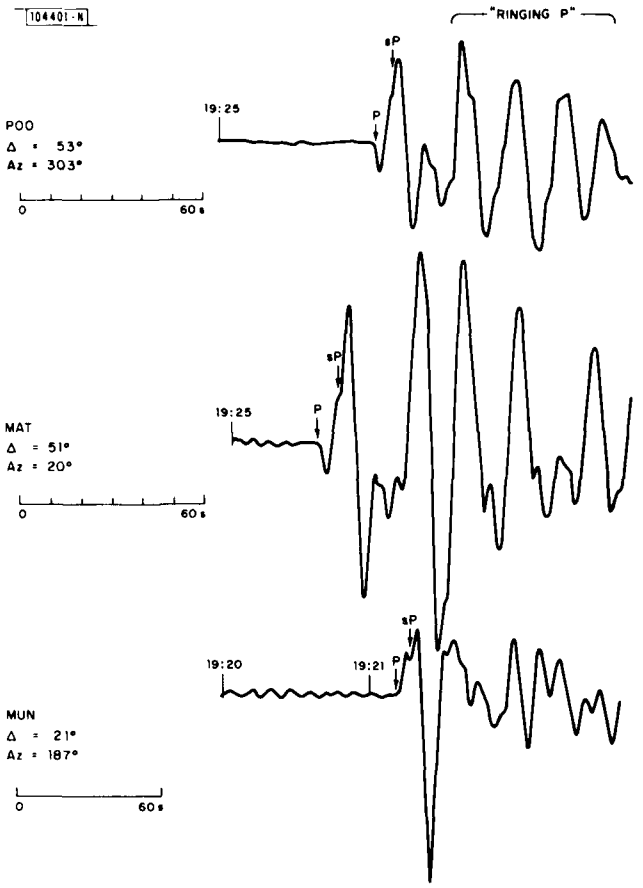

Fig. II-12. LPZ WWSSN seismograms for earthquake of 20 August 1977.

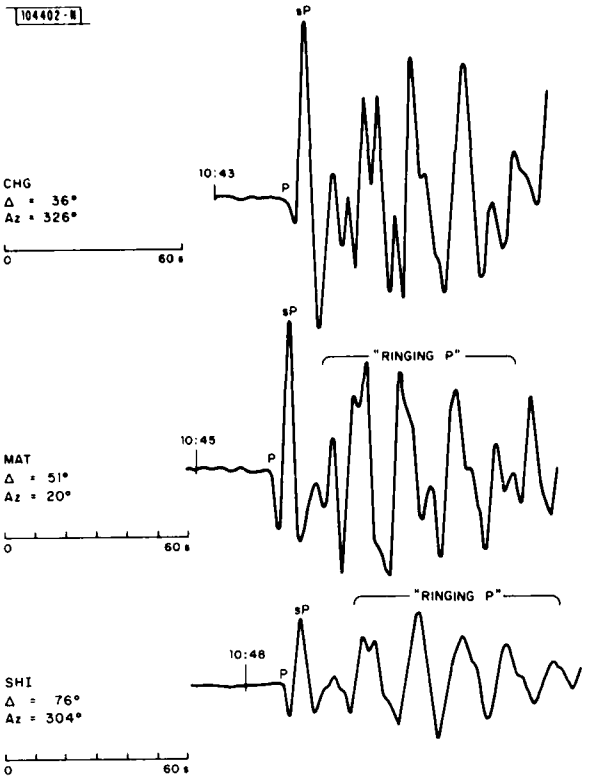

Fig. II-13. LPZ WWSSN seismograms for earthquake of 2 September 1977. P-waveforms are not offset like those of 20 August 1977, but deviate from expected response to a single impulse. Earthquake depth < 10 km.

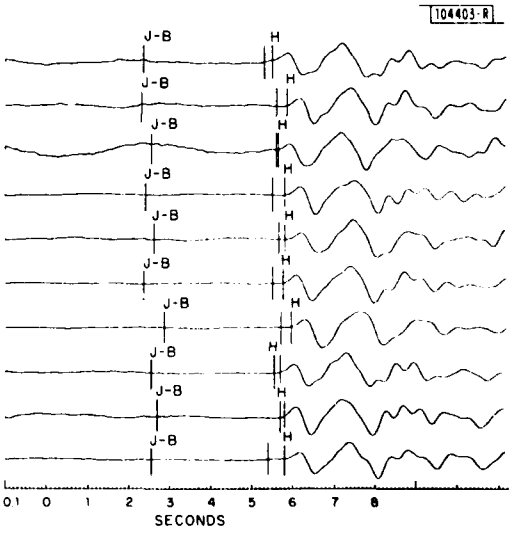

Fig. II-14. Comparison of Human (H) and Detector (no label) made picks. J-B table calculated onset times are also shown (J-B).

III. GENERAL SEISMOLOGY

A. SURFACE WAVES GENERATED BY COMBINATIONS OF EXPLOSIVE AND FAULTING SOURCES

In the preceding SATS,[1] the results of a study of SRO data from several presumed explosions in Eastern Kazakh were presented. For one of these events (7 July 1979), we found that the Rayleigh waves were reversed in phase over the entire usable period band (15 to 50 s) at all azimuths and that, in addition, the Rayleigh waves from this event displayed significant azimuthal asymmetry compared with all the other events from the same small source region. Here, we consider the character of the far-field surface radiation generated by the addition of a faulting component to the symmetric explosion source. The most convenient representation of such a combination is given by the seismic moment tensor, to which the radiation is linearly related.

The far-field Love (F_L) and Rayleigh (F_R) radiation from a source of given moment tensor is given by[2]

$$F_L = \{A_L [Mxy \cos 2\phi + 0.5(Myy - Mxx) \sin 2\phi] + iB_L [-Myz \cos \phi + Mxz \sin \phi]\} e^{i\pi/4}$$

$$F_R = \{A_R [Mxy \sin 2\phi - 0.5(Myy - Mxx) \cos 2\phi] + C_R Mzz + 0.5 A_R (Myy + Mxx) - iB_R [Myz \sin \phi + Mxz \cos \phi]\} e^{i\pi/4}$$

where A_L, B_L, A_R, B_R, and C_R are related to the displacements and stresses at the source depth h. For very shallow sources such that $(h/\lambda) \ll 1$, the stress components, entering into B_L and B_R, are very small at a given wavelength λ and vanish at the surface. Additionally, $C_R = -1/3 A_R$ close to the free surface. Consequently, at shallow depths the imaginary parts of F_L and F_R are very poorly excited, and the above expressions reduce to

$$F_L = A_L e^{-i\pi/4} [Mxy \cos 2\phi + 0.5(Myy - Mxx) \sin 2\phi]$$

and

$$F_R = A_R e^{i\pi/4} [Mxy \sin 2\phi - 0.5(Myy - Mxx) \cos 2\phi - 1/3 Mzz + 0.5(Myy + Mxx)] \quad .$$

Note that the source phase, excluding the $e^{\pm i\pi/4}$ terms, can only be 0 or Π since the imaginary part essentially vanishes, and that the shape of the spectrum is given simply by either A_L or A_R, regardless of the azimuth of observation ϕ.

For an explosive source, the moment tensor is given by equal diagonal components

$$Mxx = Myz = Mzz = M_o^e$$

producing azimuthally invariant radiation.

Following Mendiguren,[2] the tensor components for a fault aligned in the x-direction of a Cartesian (x, y, z) system are given by:

Vertical strike-slip	$Mxy = M_o^F$, others zero
Pure dip-slip	$Mxy = Mxx = 0$
	$Myy = -M_o^F \sin 2d$
	$Mzz = +M_o^F \sin 2d$
	$Myz = -M_o^F \cos 2d$
	$Mxz = +M_o^F \cos 2d$

where d is the dip of the fault plane, and $0 < d < 90$ represents thrust faulting and $90 < d < 180$ normal faulting.

In the notation of Mendiguren,[2] the far-field Rayleigh $F_R(\omega)$ and Love $F_L(\omega)$ are given as follows:

For an explosive source,

$$F_R = 2/3 A_R M_o^e$$

$$F_L = 0$$

For the vertical strike-slip source,

$$F_R = A_R M_o^F \sin 2\phi$$

$$F_L = A_L M_o^F \cos 2\phi$$

For a pure dip-slip source,

$$F_R = 1/2 A_R M_o^F \sin 2d(\cos 2\phi - 5/3)$$

$$F_L = -1/2 A_L M_o^F \sin 2d \sin 2\phi$$

where we have everywhere dropped the $e^{\pm i\pi/4}$ terms. A_L is always positive, and for shallow depths A_R is negative over the period range of interest. The source phase of the Rayleigh waves from an explosive source is thus π, and that for dip-slip faulting is 0 for $\sin 2d > 0$ (thrust) and π for $\sin 2d < 0$ (normal faulting).

We are particularly interested in combinations of explosive and faulting sources which will generate phase reversals (i.e., source phase of 0) at all azimuths ϕ, compared with the pure explosive source. The strike-slip source generates the familiar four-lobed pattern for which the source phase is alternately zero or π and the source phase for a normal fault is everywhere π. Only the thrust fault has a source phase of zero at all azimuths ϕ. A combination of the explosive and thrust-faulting sources will thus produce the desired phase reversal if

M_o^F is sufficiently large. The radiation from the thrust fault is maximized for a dip of 45°, and for this case the spectrum of such a combination is given by

$$F_R = A_R M_o^e [2/3 + 1/2 R_{FB}(\cos 2\phi - 5/3)]$$

where

$$R_{FB} = \frac{M_o^F}{M_o^e} \quad .$$

Love waves are excited only by the thrust faulting and are given by

$$F_L = \frac{A_L}{2} M_o^e R_{FB} \sin 2\phi \quad .$$

The Rayleigh- and Love-wave radiation patterns are given in Fig. III-1 for various values of R_{FB}. The Love-wave radiation pattern grows in amplitude linearly as R_{FB} increases. The Rayleigh-wave radiation patterns exhibit the interesting behavior of changing from circular (explosion) to two-lobed (normal faulting) through four-lobed (vertical strike-slip faulting) to two-lobed (thrust faulting) as R_{FB} increases. On the basis of the Rayleigh-wave radiation alone, these patterns for different types of faulting are indistinguishable from a combination of explosive and thrust-faulting sources. Note that the phase reversal at all azimuths does not occur until R_{FB} exceeds 2. The relative amplitudes of Love and Rayleigh are a function of frequency, and for a shield model[2] the Love-wave amplitudes shown should be multiplied by (1.36, 1.79, 2.17, 1.95, and 1.88) at periods of 50, 40, 30, 20 and 16 s, respectively, to correctly reflect relative Love and Rayleigh amplitudes at these periods.

It has been pointed out[3] that faulting involved with the explosive process need not involve tectonics,[4] and that fracturing along dipping planes has been observed at the NTS. Such fractures must, however, have a preferred direction to produce the features of the surface-wave radiation observed for some Eastern Kazakh explosions.[1] Thrust faulting on a conical surface above the explosive source may be modeled by considering it as a sum (or integral) over all possible fault orientations ϕ. In this case, for a pure dip-slip fault at dip angle d, orientation ϕ, we have

$$Mxy = 1/2 \sin\phi \sin 2d$$

$$Mxx = -\sin^2\phi \sin 2d$$

$$Myy = -\cos^2\phi \sin 2d$$

$$Mzz = \sin 2d$$

$$Myz = -\cos\phi \cos 2d$$

$$Mxz = \sin\phi \cos 2d$$

and

$$\int_o^{2\pi} Mxy \, d\phi = \int_o^{2\pi} Myz \, d\phi = \int_o^{2\pi} Mxz \, d\phi = 0$$

$$\int_o^{2\pi} Mxx \, d\phi = \int_o^{2\pi} Myy \, d\phi = -\Pi \sin 2d$$

$$\int_o^{2\pi} Mzz \, d\phi = 2\Pi \sin^2 d \quad .$$

The net result is a compensated linear vector dipole (CLVD) with zero Rayleigh-wave phase which does not, however, generate Love waves or any azimuthal variation in the Rayleigh-wave radiation. These last two features require a preferred orientation of faulting which may be conditioned by either pre-existing stress or planes of weakness in the source region.

We plan to investigate further the character of surface-wave radiation, with particular emphasis upon the Love waves, from explosive sources.

The effect of the combined explosion/thrust faulting upon M_s is summarized in Fig. III-2 which shows the maximum, minimum, and average (over azimuth) for field Rayleigh-wave amplitudes as a function of R_{FB}. The last may be considered to reflect the average M_s computed from a number of stations, and can be seen to possess a minimum of one-third that from the pure explosion at $R_{FB} = 0.6$. This corresponds to a reduction in M_s of about 0.5 unit, which is certainly significant in M_s-yield calculations.

R. G. North
T. J. Fitch

B. MEASUREMENT OF DISPERSION AND ATTENUATION OF MANTLE WAVES THROUGH LINEARIZED INVERSION OF WAVEFORM DATA: I. THEORY AND A TEST ON SYNTHETIC DATA

Much of our current knowledge on the distribution of shear velocity and attenuation in the upper mantle comes from the studies of surface waves. So-called mantle waves have periods greater than 100 s and are attenuated slowly enough that it is possible to observe at a given station several of their consecutive passages around the world. These LP waves are now routinely detected by modern instruments for events of a surface-wave magnitude as low as 6.5. In addition to their important role in providing constraints on the mantle structure in a depth range from 100 to 400 km, they are also used in source mechanism studies. Precise knowledge of phase velocities is needed in inversion of waveform data for the seismic moment tensor.

The principle of measuring the phase velocity and attenuation from observations of mantle waves is very simple. The spectral ratio of two wave groups whose paths differ by one circumference yields a spectrum of transfer function $T(\omega)$ that in the time domain corresponds to the shape of a δ-function signal after one complete passage around the Earth[5]

$$T(\omega) = R_{n+2}(\omega)/R_n(\omega) \quad . \tag{III-1}$$

The spectrum of $T(\omega)$ must be of the form:

$$T(\omega) = \exp\left[-2\pi a \left\{ i \left[k(\omega) - \frac{1}{2a} \right] + \frac{\omega q(\omega)}{2u(\omega)} \right\}\right] \tag{III-2}$$

where $k(\omega)$ is the wave number, $u(\omega)$ is the group velocity, and $q(\omega)$ is the inverse of the quality factor Q. Thus, the analysis of the phase of the $T(\omega)$ allows the wave number to be determined as a function of frequency and its amplitude yields $Q(\omega)$, if the group velocity is known. The frequencies of zero crossings of the phase spectrum correspond to the frequencies of free oscillations of the Earth.

In practice, direct application of Eq. (III-1) leads to serious difficulties, as the process of deconvolution, implied by the ratio of two spectra contaminated by the noise and energy of overtones, leads to unstable results even for a limited range of frequencies.

Nakanishi[6] derived the $T(\omega)$ through a design of the Wiener filter, but it appears that this procedure may also lead to physically unacceptable results; the $T(\omega)$ shown in his Fig. 2a cannot be a functional of a realistic Earth model.

We intend to make use of the fact that the $T(\omega)$ must be consistent with a reasonable Earth structure; this is equivalent to using the known properties of the Earth as a smoothing filter. The most direct way to assure that this condition is satisfied is to derive the $T(\omega)$ through the process of perturbation of structural parameters of a selected starting Earth model.

We shall attempt to find a $T(\omega)$ that satisfies the following least-squares condition:

$$\int_{\omega_1}^{\omega_2} |R_{n+2}(\omega) - R_n(\omega) \cdot T(\omega)|^2 \, d\omega = \min \quad . \tag{III-3}$$

Let the $T(\omega)$ computed for the starting model be $T^0(\omega)$. It is characterized by a complex function $K^{(0)}(\omega)$, closely related to the complex wave number and corresponding to the expression within the braces in Eq. (III-2). Thus,

$$T^0(\omega) = \exp[-2\pi i a K^0(\omega)] \quad . \tag{III-4}$$

A small perturbation in the structural parameters of the starting model will lead to a change in $K^0(\omega)$ that can be evaluated using the linear perturbation theory[7]:

$$\delta K^0(\omega) = \int_0^1 \underline{G}^0(r, \omega) \cdot \delta \underline{m}(r, \omega) \, dr \tag{III-5}$$

where the differential kernels $\underline{G}^0$ and the Earth model $\underline{m}$ may both be complex. The effect of attenuation on velocity dispersion[8] may be incorporated in Eq. (III-5). If the change in $\delta \underline{m}$ is very small, then we may write

$$\exp[-2\pi i a \delta K^0(\omega)] \sim 1 - 2\pi i a \delta K^0(\omega) = 1 - 2\pi i a \int_0^1 \underline{G} \cdot \delta \underline{m} dr \quad . \tag{III-6}$$

The integral over a finite frequency range in Eq. (III-3) may be changed to a sum over the discrete elements of the spectrum, and upon substitution of Eq. (III-6) the least-squares condition becomes

$$\sum_j |R_{n+2}(\omega)_j - R_n(\omega)_j T_j^0 + 2\pi i a R_n(\omega)_j T_j^0 \int_0^1 \underline{G}_j \cdot \delta \underline{m} dr|^2 = \min \quad . \tag{III-7}$$

The inverse problem for $\delta \underline{m}(r)$ posed by Eq. (III-7) can be solved either in the data or parameter space using one of many methods described in the literature. It is important, however, that the perturbation estimated in each iteration be small enough that the approximation assumed in Eq. (III-6) is valid. For this reason, it will be generally necessary to damp the inverse heavily and perform several iterations. After each iteration, the $T(\omega)$ is recalculated exactly:

$$T^{(j)}(\omega) = T^{(j-1)} \exp[-2\pi i a \delta K^{(j)}] \quad . \tag{III-8}$$

After the convergence is achieved, it is prudent to recompute function $K(\omega)$ and the differential kernels for the new model and repeat the entire process.

Another difficulty in estimation of the $T(\omega)$ is that the wavegroups corresponding to the individual orbits cannot always be readily isolated. Clearly, when the receiver is close to the source or its antipodes, then the energy of odd- and even-numbered wavegroups will overlap. However, even at the optimal distance of 90°, a 500-s wave of R_5 will arrive at the same time

as a 220-s wave of R_4. For this reason, the most reliable measurements of dispersion and attenuation of mantle waves have been limited to the period range for 150 to 300 s - the interval in which both Rayleigh and Love waves are weakly dispersed.

The development of the technique described above, which does not require estimation of the spectral ratio but relies on minimizing the difference between two functions of time or frequency, allows us to reformulate the approach to the analysis of mantle waves.

Consider that a seismogram consists of a series of arrivals of wavegroups: $R_1, R_2, R_3, R_4, \ldots, R_n$. Convolution of such a seismogram with the transfer function T transforms it into a series $R_3, R_4, R_5, \ldots, R_n$. The difference between these two series is $R_1 + R_2$, a signal of finite duration t_1, determined by the slowest group velocity of the wavegroup R_2. The remainder of the trace is identically zero, if the transfer function T corresponds to that for the real Earth. In practice, we shall be dealing with seismograms of finite duration truncated, say, at a time t_2. Thus, the operation described above is equivalent to

$$S(t) - S(t) * T(t) = 0 \quad \text{for } t_1 \leq t \leq t_2 \quad . \tag{III-9}$$

In the frequency domain, the least-squares condition thus will be

$$\int_{\omega_1}^{\omega_2} \left| F\,[S(t)]_{t_{1,2}} - F\,[S(t) * T(t)]_{t_{1,2}} \right|^2 d\omega = \min \tag{III-10}$$

where F is the Fourier transform and the subscript indicates that the transform is evaluated for the time interval from t_1 to t_2. Further procedure is identical to that described above for a pair of the wavegroups.

What has been gained is that we can use the signal contained in an entire seismogram and that we completely bypass the problem associated with overlapping energy of wavegroups belonging to different orbits. It is not necessary that the analyzed seismogram should begin with the first minor arc arrival R_1. It may begin at any time t_0, providing that the interval t_1 to t_0 is sufficiently long; 190 min., the circumferential travel time of the slowest mantle Rayleigh waves, is a conservatively safe estimate.

The entire procedure has been tested first on synthetic data; application to the analysis of observed seismograms is described in Sec. C below. The synthetic seismogram shown in Fig. III-3 has been obtained by superposition of the fundamental spheroidal modes computed for an Earth model perturbed by the amounts listed in Table III-1 with respect to the reference model. The objective of this test is to find out how well our procedure will perform in determining the values of these perturbations if we use the transfer function T for the reference model in the starting iteration. The test is a rather difficult one, as the perturbations in the shear velocity offset each other.

The top trace in Fig. III-4(a) is the "observed" seismogram displayed for the time interval corresponding to the box in Fig. III-3. The next trace is the result of convolution of the complete seismogram of Fig. III-3 with the transfer function for the starting model. Even visual inspection reveals that there are substantial differences between these two time functions. Their values are displayed in the third trace and, indeed, the amplitudes in the difference trace are comparable to those of the signal. Despite the magnitude of differences, the procedure converges, and the bottom trace shows that the residual function

$$[S(t) - S(t) * T(t)]_{t_{1,2}}$$

TABLE III-1

PERTURBATIONS TO THE REFERENCE MODEL USED IN THE SYNTHETIC TEST[†]

Depth Range (km)	Δv_s (km/s)	Δq_μ
19 to 80	0.1	−0.0030
80 to 220	0.1	0.0025
220 to 400	0.1	−0.0032
400 to 670	−0.1	−0.0022

† The Earth model used to generate the synthetic seismogram shown in Fig. III-3 was obtained by perturbing the shear velocities and attenuation of model PREM of Dziewonski and Anderson[9] by the amounts listed above. Through the linearized inversion of the seismogram in Fig. III-3 we shall attempt to recover these values, using the transfer function computed for PREM in the starting iteration. The quantity q is the reciprocal of the quality factor Q.

is very small and, therefore, our transfer function obtained as the result of inversion should represent the "true" dispersion and attenuation rather well. The frequency-domain equivalent of Fig. III-4(a) is shown in Fig. III-4(b), where the moduli of the spectral amplitudes are displayed.

Throughout all iterations that led to the final result, the differential kernels $G(r,\omega)$ were kept unchanged, even though they are functionals of the model and the model changed during inversion. It is desirable to recompute the eigenfrequencies and differential kernels after the first pass, and repeat the entire process. Figure III-5 demonstrates that the effect of the nonlinearity is discernible. The starting transfer function is now computed for the final model of "Pass 1." Note that amplitudes of the difference at the beginning of Pass 2 are greater than at the end of Pass 1. This means that the effect of nonlinearity is important if one considers derivation of the Earth model to be the principal objective of the procedure. If only measurement of dispersion and attenuation is of importance, then the accuracy of the result obtained at the end of Pass 1 will be sufficient for practical purposes.

Figure III-6(a) shows comparison of the phase velocities measured after Passes 1 and 2 with the exact results; the largest difference after Pass 1 is about 5 parts in 100,000, and after Pass 2 the results agree to five significant figures. The differences in attenuation, shown in Fig. III-6(b), are more substantial and for Pass 1 they reach 2 percent at 600 s. One can expect, however, that the magnitude of this error caused by the nonlinearity of the procedure is small in comparison with other sources of error that would be encountered in processing actual data.

In Fig. III-7(a-b) we compare the retrieved structures with the known perturbation. The velocities after Pass 1 are very close to the correct answer - the largest deviation is 0.01 km/s or 10 percent of the perturbation. However, there are major differences in the Q structure; in particular, the sign of the perturbation in the lid is opposite to the correct one. The structure derived in Pass 2 is extremely close to the true structure.

There are immediate applications of the technique described in this report and they will be presented in Sec. C below. There is certain conceptual affinity between the developments presented here and the approach adopted by Dziewonski et al.[10] in their study of earthquake source parameters. In both cases, the direct inversion of waveform data results in derivation of parameters that in the past required an intermediate stage of the analysis. It is perhaps not unrealistic to think that in the not-too-distant future one will be able to process a large set of recordings from many earthquakes, determine their hypocentral parameters, source mechanisms, and, at the same time, derive an improved model of the laterally heterogeneous Earth.

A. M. Dziewonski

C. SIMULTANEOUS RETRIEVAL OF DISPERSION AND ATTENUATION OF MANTLE WAVES THROUGH LINEARIZED INVERSION OF WAVEFORM DATA: II. APPLICATION TO ANALYSIS OF SEISMOGRAMS FROM THE IDA NETWORK

In Sec. B above, we outlined the principle of the measurement of phase velocities and Q of the fundamental mode mantle waves from recordings of arbitrary length. It is our opinion that there are two essential advantages of the proposed method over the past techniques: (1) usage of the properties of the Earth as a smoothing filter yields dispersion curves that do not contain physically unrealistic features, and (2) the signal-to-noise ratio and the frequency range of measurements are increased because truncation necessary to isolate the individual wavegroups is avoided and data for many pairs of the wavegroups are used simultaneously. It is also possible to obtain estimates of the source parameters. The dispersion and attenuation of the Rayleigh and Love waves, although so far we have not used this opportunity in the analysis of observed data.

It is possible to think of immediate extensions of the theory presented in Part I (see Sec. B above), for example, it could be used to measure the phase velocity and attenuation between two stations on the same great circle with the source. But, in addition, we feel that the conceptual aspects of our approach — derivation of model parameters directly from waveform data — may have potential for much broader applications in seismological research.

Data from the network of the International Deployment of Accelerometers[11] (IDA) provide an excellent opportunity to test our method of determination of the transfer function. The response of these instruments is designed to enhance the energy at long periods, and even visual examination of the records allows us to appreciate the significant amplitudes of waves with periods in excess of 500 s, seldom detectable in the recordings of the WWSSN stations for events with magnitude less than 7.5.

Figure III-3 shows a recording of an event near the Solomon Islands (29 July 1977) obtained at Halifax, Nova Scotia. The original recording has been processed with a low-pass filter of a cutoff period of 150 s. The first wavegroup identified in this figure is R_3, the amplitudes of R_1 and R_2 exceeded the range of linearity of the instrument. This recording most likely would not have been used in the standard analysis, as the closeness of the arrivals R_3 and R_4 makes the necessary separation of these and subsequent wavegroups very difficult. This figure is an equivalent of Fig. III-1, with the difference that the time series shown here does not begin at the origin time.

The difference trace in Fig. III-3a shows that the transfer function for the reference model decreases perceptibly from that appropriate for this path. There is a clear correlation between the large amplitudes of the difference trace and the occurrence of the wavegroups in the observed seismograms. However, after inversion, the envelope of the difference signal decreases smoothly

with time; the gradual decrease in the frequency content suggests that it represents an attenuated seismic signal, most likely associated with the energy of overtones. The equivalent trace in Fig. III-9(b), representing the power spectrum of the residual trace, indicates that no correlation with the spectral peaks of the fundamental spheroidal mode remains. We have demonstrated, therefore, that the method does indeed succeed in properly modifying the transfer function through perturbation of the structural parameters.

The purpose of Fig. III-10 is to demonstrate that dispersion measured in such a way is in general agreement with the results obtained using standard techniques. The continuous lines in that figure represent results of phase-velocity measurements obtained from the phase-delay function of the appropriately selected fragment of the autocorrelogram of the observed seismogram[12]; the smooth broken lines are the values resulting from application of the technique described in this report. It is clear that there is an overall correspondence between these two sets of answers; the smooth lines represent the trend of the results from the phase delay analysis, but, in addition to being physically realistic, they also extend to substantially longer periods.

Figure III-11 demonstrates the repeatability of the results. Two strong earthquakes in the Solomon Islands (M_S 6.9 and 7.3) occurred within 22 h of each other; their locations were extremely close, and visual inspection of several recordings indicates that their source mechanisms were also similar. The dispersion curves shown in Fig. III-9(a) are identical for a large range of angular order numbers, and the maximum difference at short periods is of the order of 0.03 percent. This agreement is even more remarkable, as the delay with respect to the origin time was different for the two earthquakes because of the difference in their magnitude.

By a remarkable coincidence, we have found recordings of three earthquakes on nearly the same great-circle path with a station at Ñaña, Peru (see Fig. III-12); the poles of the individual paths are within 100 km of each other. Unlike in the case shown in Fig. III-11, the locations of the events were quite different. We do not know the source mechanisms of these earthquakes, but it is highly unlikely that they would be similar. Although there is an overall similarity between the three dispersion curves, the differences are several times greater than the maximum difference in Fig. III-11. This effect can be explained by the results of Woodhouse, presented in Sec. D below. It shows that the perturbation in the period of a particular normal mode depends, in general, on the location of the source and receiver as well as on the source mechanism.

We have obtained results for 37 great-circle paths and performed decomposition of the observed phase velocities and attenuation in terms of the geometrical "pure path" analysis first proposed by Toksöz and Anderson,[13] and later used by Kanamori[14] and Dziewonski[15] as well as several other authors.

Stable results were obtained to periods as long as 600 s, roughly twice the range achieved in the earlier analyses. However, it appears from the work of Woodhouse that there is a distinct possibility that the geometrical ray approximation may lead to serious errors, particularly at very long periods (wavelengths). For this reason, we do not think that publication of our current results would be particularly useful.

A. M. Dziewonski
J. M. Steim†

† Department of Geological Sciences, Harvard University.

D. A NONASYMPTOTIC "RAY THEORY" FOR SURFACE WAVES AND FREE OSCILLATIONS

The effect of lateral heterogeneities on the dispersion of surface waves is known to be substantial in the Earth, and has been the subject of many studies.[12-15] The interpretation of such dispersion data invariably has been performed under the assumption that the dispersion characteristics are those appropriate for a model with the structure which is the average of the true structure along the great-circle path for which the data were obtained. For a given regionalization of the Earth, this ray theoretic approximation enables one to invert for the dispersion characteristics of each region, assumed uniform, and thus to quantify the variations in structure among the regions. We shall refer to this approach as the "pure path" technique.

Another approach to the treatment of the effects of lateral heterogeneity is through the theory of spectral splitting of free oscillations.[16-18] We shall refer to this as the "splitting technique," though it is a technique which has not been applied to actual data.

It has been shown by Jordan[18] that a convenient connection between the two techniques may be established through the spectral "location parameter" λ, namely the difference in frequency between the centroid of a spectral peak corresponding to a given (fundamental) normal mode and the corresponding eigenfrequency of a reference Earth model. In particular, it has been shown[18] that asymptotically, in the limit of large angular order, the location parameter for a particular source and receiver is simply the average along the appropriate great-circle path of $\delta\omega_{\text{local}}$, which is defined at each point of the globe (θ, ϕ) as the frequency shift appropriate for a spherical model possessing the structure locally beneath that point (the angles θ, ϕ will be used to denote colatitude and longitude, respectively). This result provides the theoretical justification for the pure path technique, and is intuitively very appealing. In order to obtain it, however, severe approximations must be made. In particular, it must be assumed that the wavelengths characteristic of the lateral variations in structure are much longer than those of the surface-wave mode under consideration, a situation which probably does not obtain in the Earth; indeed, a remarkable and graphic demonstration of the inadequacy of the ray theoretic approximation, using data from the IDA network, is presented by Dziewonski and Steim in Sec. C above.

It is the purpose of this report to show that the result from the theory of splitting for the spectral location parameter may be recast, without any further assumptions, into a form similar to that used in the pure path technique. The difference is that, instead of depending only upon $\delta\omega_{\text{local}}$, λ depends upon three local functionals of Earth structure $\{\delta\omega^{(i)}(\theta, \phi),\ i = 1, 3\}$ and, in addition, the path average must be performed using not the geometrical path lengths in each region but three other parameters which are fairly readily calculated, and for which formulas will be given. Thus, it is possible to quantify the effect on the location parameter of regional structural variations in a manner which is similar to that assumed in the pure path technique, but which does not involve the approximations entailed by that technique.

We shall confine our attention here to a particular free oscillation multiplet ${}_nS_\ell$ or ${}_nT_\ell$ where n is radial order, ℓ is angular order, and S and T refer to spheroidal and toroidal modes, equivalently, we shall consider a Rayleigh or Love wave at some particular wavelength.

From the theory of splitting, it may be shown[18] that for a given source-receiver pair the location parameter is given by

$$\lambda = \frac{1}{p} \sum_{mm'} R^{m'} S^{m} H_{m'm} \qquad \text{(III-11)}$$

with

$$p = \sum_{m} \cdot R^{m} S^{m'}$$

where the summations are over azimuthal order for $-\ell \leq m,\ m' \leq \ell$. In Eq. (III-11), $R^{m'}$ will be referred to as the receiver vector and is given by

$$R^{m'} \quad R^{m'}(\theta_r, \phi_r) = \sum_{N=-1}^{1} R_N Y_\ell^{Nm}(\theta_r, \phi_r) \tag{III-12}$$

and S^m will be referred to as the source vector, and is given by

$$S^m = S^m(\theta_s, \phi_s) \equiv \sum_{N=-2}^{2} S_N Y_\ell^{Nm}(\theta_s, \phi_s) \quad . \tag{III-13}$$

In Eqs. (III-12) and (III-13), $Y_\ell^{Nm}(\theta, \phi)$ are the generalized spherical harmonics of Phinney and Burridge,[19] and θ_r, ϕ_r, θ_s, and ϕ_s are the colatitude and longitude of receiver and source. $R_N \equiv R^N(0, 0)$, $S_N \equiv S^N(0, 0)$ depend upon the orientation of the component measured by the seismometer and the moment tensor of the source, respectively, and are given in Table III-2. In Eq. (III-11), $H_{m'm}$ are components of the splitting matrix.[16,17] The splitting matrix will involve components dependent upon the Earth's rotation and ellipticity $H_{m'm}^{(re)}$, together with those relating to the difference between the reference Earth model and the actual Earth. $H_{m'm}^{(re)}$ is readily calculated, and here we shall be concerned with only the remaining terms. Therefore, we shall write

$$H_{m'm} = H_{m'm}^{(re)} + \tilde{H}_{m'm} \quad .$$

Let us suppose now that the Earth differs from the reference model by amounts $\delta\rho$, $\delta\kappa$, $\delta\mu$, $\delta\phi_0$, $\delta\partial_r\phi_0$ in density, bulk modulus, shear modulus, gravitational potential, and its radial derivative, respectively, and let us denote these model perturbations by the vector $\delta\underline{m} = \delta\underline{m}(r, \theta, \phi)$ The perturbations may be expanded in spherical harmonics:

$$\delta\underline{m} = \sum_{st} \delta\underline{m}_s^t Y_s^t(\theta, \phi) \quad .$$

Woodhouse and Dahlen[17] have given expressions for $\tilde{H}_{m'm}$ in terms of $\delta\underline{m}_s^t(r)$, which we need not repeat here except to note that they take the following form:

$$\tilde{H}_{mm'} = \sum_{st} \gamma_s^{mm't} \int \delta\underline{m}_s^t(r) \cdot \{\underline{M}^{(0)}(r) + s(s+1)\, \underline{M}^{(1)}(r) + [s(s+1)]^2\, \underline{M}^{(2)}(r)\}\, r^2 dr \tag{III-14}$$

TABLE III-2

COEFFICIENTS FOR EVALUATING THE SPECTRAL LOCATION PARAMETER

N	$R_N \equiv R^N(0,0)$	$S_N \equiv S^N(0,0)$
0	$k_0 U v_r$	$k_0[\partial_r U M_{rr} + 1/2\, F(M_{\theta\theta} + M_{\phi\phi})]$
±1	$k_1(V \pm iW)(\mp v_\theta - iv_\phi)$	$k_1(X \pm iZ)(\mp M_{r\theta} - iM_{r\phi})$
±2	–	$k_2 r_s^{-1}(V \pm iW)[(M_{\theta\theta} - M_{\phi\phi}) \pm 2iM_{\theta\phi}]$
U, V, W are scalar eigenfunctions[20] evaluated at the Earth's surface		U, V, W are scalar eigenfunctions[20] evaluated at the source radius r_s
$k_n = \frac{1}{2^n}\left[\frac{2\ell+1}{4\pi} \cdot \frac{(\ell+n)!}{(\ell-n)!}\right]^{1/2}$		$F = r^{-1}[2U - \ell(\ell+1)V]$ $X = \dot{V} + r^{-1}(U - V)$ $Z = \dot{W} - r^{-1}W$

NOTES: M_{rr}, $M_{r\theta}$, etc. are components of the moment tensor.

v_r, v_θ, v_ϕ are components of the "instrument vector." Viz. a unit vector in the direction of motion sensed by the instrument, multiplied by the instrument response.

Dot denotes differentiation with respect to radius r.

where $\underline{M}^{(i)}(r)$ are given by known expressions in terms of scalar eigenfunctions and, what is important here, are independent of s. The coefficients $\gamma_s^{mm't}$ are

$$\gamma_s^{mm't} = \int Y_\ell^{m*} Y_s^t Y_\ell^{m'} \, d\Omega$$

where the integration is over the unit sphere.

Now, if $\underline{\nabla}_1$ denotes the gradient operator on the sphere:

$$\underline{\nabla}_1 = \hat{\underline{\theta}}\partial_\theta + \operatorname{cosec}\theta \, \hat{\underline{\phi}}$$

we may use the divergence theorem on the sphere to write

$$\sum_{st} [s(s+1)]^i \gamma_s^{mm't} \delta\underline{m}_s^t(r) = \sum_{st} \delta\underline{m}_s^t(r) \int Y_s^t(-\nabla^2)^i (Y_\ell^{m*} Y_\ell^{m'}) \, d\Omega$$

$$= \int \delta\underline{m}(r, \theta, \phi)\, k_i^{mm'}(\theta, \phi) \, d\Omega$$

with

$$k_i^{mm'}(\theta, \phi) = (-\nabla_1^2)^i \, Y_\ell^{m*} Y_\ell^{m'}$$

and Eq. (III-14) becomes

$$\tilde{\Pi}_{mm'} = \sum_{i=0}^{2} \iiint \delta\underline{m}(\mathbf{r}, \Theta, \phi)\, k_i^{mm'}(\Theta, \phi)\, r^2 dr d\Omega$$

and the location parameter is given by

$$\tilde{\lambda} = \sum_{i=0}^{2} \int \delta\omega^{(i)}(\Theta, \phi)\, K_i(\Theta, \phi)\, d\Omega \qquad \text{(III-15)}$$

with

$$K_i(\Theta, \phi) \equiv \frac{\sum_{mm'} R^{m'} S^{m*} k_i^{m'm}(\Theta, \phi)}{[2\ell(\ell+1)]^i \sum_{m} R^m S^{m*}}$$

$$\delta\omega^{(i)}(\Theta, \phi) \equiv [2\ell(\ell+1)]^i \int \underline{\delta m}(r, \Theta, \phi) \cdot \underline{M}^{(i)}(r)\, r^2 dr \quad .$$

The factors $[2\ell(\ell+1)]^i$ have been introduced to normalize the kernels in a convenient, but somewhat arbitrary, way.

Equation (III-15) is the principal theoretical result of this report, and states that $\tilde{\lambda}$ is given by the weighted average over the surface of the Earth of three local functionals of Earth structure, $\delta\omega^{(i)}$, with respect to kernels which are readily calculated, provided source and receiver are known. $\delta\omega^{(0)}$ is identical to $\delta\omega_{local}$ of Jordan.[18]

The kernels $K_i(\Theta, \phi)$ are most easily evaluated by making use of a coordinate system in which the point (Θ, ϕ) is located at the pole. It may then be shown that

$$K_i(\Theta, \phi) = \frac{1}{p} \left(\frac{2\ell+1}{4\pi}\right) \sum_{NMN'} a_i^M S_{N'}^* R_N P_\ell^{N'M}(\Delta_{ps})\, P_\ell^{NM}(\Delta_{pr})$$

$$\times \exp\{i\,[N\phi_{pr} - N'\phi_{ps} + M(\phi_{sp} - \phi_{rp})]\}$$

where a_i^M are given in Table III-3, and P_ℓ^{NM} are generalized associated Legendre functions.[19] The angles Δ, ϕ are:

Δ_{ps} = angular distance of (Θ, ϕ) from (Θ_s, ϕ_s)

Δ_{pr} = angular distance of (Θ, ϕ) from (Θ_r, ϕ_r)

ϕ_{ps} = azimuth of (Θ, ϕ) from (Θ_s, ϕ_s)

ϕ_{pr} = azimuth of (Θ, ϕ) from (Θ_r, ϕ_r)

ϕ_{sp} = azimuth of (Θ_s, ϕ_s) from (Θ, ϕ)

ϕ_{rp} = azimuth of (Θ_r, ϕ_r) from (Θ, ϕ).

TABLE III-3

COEFFICIENTS FOR EVALUATING THE PATH FRACTION KERNELS

	a_i^M		
	M = 0	M = ±1	M = ±2
i = 0	1	–	–
i = 1	1	−1/2	–
i = 2	3/2	$[2\ell(\ell+1)]^{-1} - 1$	$1/4 - [2\ell(\ell+1)]^{-1}$

Since the summations over M, N' are only from −2 to +2, and those over N from −1 to +1, the kernels can be rapidly computed. Indeed, for a vertical instrument and an explosive source, K_0 is simply proportional $P_\ell(\cos\Delta_{ps})\ P_\ell(\cos\Delta_{pr})$, where P_ℓ are Legendre polynomials.

Some examples of these kernels $K_0(\Theta, \phi)$ are depicted in Figs. III-13(a) through (c). These figures represent the surface $z = K_0(\Theta, \phi)$ plotted over a Mercator projection of the Earth's surface, in which a source and a vertical instrument lie on the equator, a distance of 108° apart. The source is located at the rightmost (i.e., eastmost) end of the plots; the location of the source and receiver and their antipodes are evidenced by the peaks in Figs. III-13(a) and (c). For ${}_0S_{45}$ [Fig. III-13(c) shows the kernel for an explosive source], it is clear that the ray theoretic result of Jordan[18] is emerging; the surface wave averages local structure along the great-circle path (in this case, the equator), since over the rest of the Earth the rapid oscillations will tend to cancel in the integral. It is notable, however, that the kernel is still very broad, and does not become uniformly small toward the poles, as might have been expected on the basis of the asymptotic result. At lower frequencies it is clear that very significant deviations from ray theory can occur, and that they will depend upon source and receiver locations, and also upon the orientation of the instrument and upon the source mechanism. This last is illustrated by Figs. III-13(a) and (b), in which the only difference is that in the first the source is explosive, whereas in the second it is vertical strike slip faulting at an angle 45° to the equator.

Let us now suppose that the heterogeneous Earth comprises J laterally homogeneous regions R_j. Then we have

$$\tilde{\lambda} = \sum_{i=0}^{2} \sum_{j=1}^{J} p_j^{(i)} \delta\omega_j^{(i)} \qquad \text{(III-16)}$$

where $\delta\omega_j^{(i)}$ are those appropriate to the j^{th} region and

$$p_j^{(i)} = \int_{R_j} K_i(\Theta, \phi)\, d\Omega \quad .$$

We may refer to $p_j^{(i)}$ as the path fraction of the i^{th} kind for the j^{th} region. Indeed, if the path fraction of the zeroth kind is replaced by the geometrical path fraction for the j^{th} region, and

the path fractions of the first and second kinds are neglected, Eq. (III-16) reduces to Jordan's[18] asymptotic result – the pure path approximation. The significance of Eq. (III-16) is that the data may be interpreted in a way exactly analogous to the pure path technique, without making any approximations beyond those inherent in perturbation theory.

Let us define the functions $n_j(\Theta, \phi)$ to be unity in the j^{th} region, and zero elsewhere. If these functions are expanded in spherical harmonics:

$$n_j(\Theta, \phi) = \sum_{st} n_{js}^t Y_s^t(\Theta, \phi) \quad .$$

We obtain the following expression for the path fractions:

$$p_j^{(i)} = \frac{1}{p} \sum_{msm'} R^{m'}(\Theta_r, \phi_r)\, S^{m*}(\Theta_s, \phi_s) \left[\frac{s(s+1)}{2\ell(\ell+1)}\right]^i$$

$$\times (-1)^{m'} (2\ell + 1) \left(\frac{2s+1}{4\pi}\right)^{1/2} \begin{pmatrix} \ell & \ell & s \\ 0 & 0 & 0 \end{pmatrix} \begin{pmatrix} \ell & \ell & s \\ -m' & m & m-m' \end{pmatrix} n_{js}^{m-m'}$$

where Wigner 3-j symbols[21] have been introduced. While the evaluation of the quantities $p_j^{(i)}$ is somewhat intricate, it is not expensive computationally and we have developed algorithms for their calculation. Work proceeds on using these parameters in the interpretation of dispersion data.

J. H. Woodhouse
T. P. Girnius†

REFERENCES

1. Seismic Discrimination SATS, Lincoln Laboratory, M.I.T. (31 March 1980), DTIC AD-A091107.
2. J. A. Mendiguren, "Inversion of Surface Wave Data in Source Mechanism Studies," J. Geophys. Res. 82, 889-894 (1977).
3. R. Masse, "A Seismic Source Model for Underground Nuclear Explosions," AFTAC Special Report, AFTAC-TR-80-26 (1980).
4. M. N. Toksöz and H. H. Kehrer, "Tectonic Strain Release by Underground Nuclear Explosions and its Effect on Seismic Discrimination," Geophys. J. R. Astr. Soc. 31, 141-161 (1972).
5. A. Dziewonski and M. Landisman, "Great Circle Rayleigh and Love Wave Dispersion from 100 to 900 Seconds," Geophys. J. R. Astr. Soc. 19, 37-91 (1970).
6. I. Nakanishi, "Phase Velocity and Q of Mantle Waves," Geophys. J. R. Astr. Soc. 58, 35-59 (1979).
7. G. Backus and F. Gilbert, "Numerical Applications of a Formalism for Geophysical Inverse Problems," Geophys. J. R. Astr. Soc. 13, 247-276 (1967).

† Harvard University, now at the Department of Applied Mathematics, California Institute of Technology.

8. H-P. Liu, D. L. Anderson, and H. Kanamori, "Velocity Dispersion Due to Anelasticity: Implications for Seismology and Mantle Composition," Geophys. J. R. Astr. Soc. 47, 41-58 (1976).

9. A. M. Dziewonski and D. L. Anderson, "A Proposal for an Interim Reference Earth Model," a report submitted to the Standard Earth Model Committee of the I.U.G.G., Canberra, Australia (December 1979).

10. A. M. Dziewonski, T-A. Chou, and J. H. Woodhouse, "Determination of Earthquake Source Parameters from Waveform Data for Studies of Global and Regional Seismicity," Journal of Geophysical Research (in press, 1981).

11. D. Agnew, J. Berger, R. Buland, W. Farrel, and F. Gilbert, "International Deployment of Accelerometers: A Network of Very Long Period Seismology," Trans. Am. Geophys. Un. EOS 57, 180-188 (1976).

12. A. Dziewonski and M. Landisman, "Great Circle Rayleigh and Love Wave Dispersion from 100 to 900 Seconds," Geophys. J. R. Astr. Soc. 19, 37-91 (1970).

13. M. N. Toksöz and D. L. Anderson, "Phase Velocities of Long Period Surface Waves and Structure of the Upper Mantle: 1. Great Circle Love and Rayleigh Wave Data," J. Geophys. Res. 71, 1649-1658 (1966).

14. H. Kanamori, "Velocity and Q of Mantle Waves," Phys. Earth Plan. Int. 2, 259-275 (1970).

15. A. M. Dziewonski, "On Regional Differences in Dispersion of Mantle Rayleigh Waves," Geophys. J. R. Astr. Soc. 22, 289-325 (1971).

16. F. A. Dahlen, "Inference of the Lateral Heterogeneity of the Earth from the Eigenfrequency Spectrum: A Linear Inverse Problem," Geophys. J. R. Astr. Soc. 38, 143-167 (1974).

17. J. H. Woodhouse and F. A. Dahlen, "The Effect of a General Aspherical Perturbation on the Free Oscillations of the Earth," Geophys. J. R. Astr. Soc. 53, 335-354 (1978).

18. T. H. Jordan, "A Procedure for Estimating Lateral Variations from Low-Frequency Eigenspectra Data," Geophys. J. R. Astr. Soc. 52, 441-455 (1978).

19. R. A. Phinney and R. Burridge, "Representation of the Elastic-Gravitational Excitation of a Spherical Earth Model by Generalized Spherical Harmonics," Geophys. J. R. Astr. Soc. 34, 451-487 (1973).

20. F. Gilbert and A. M. Dziewonski, "An Application of Normal Mode Theory to the Retrieval of Structural Parameters and Source Mechanisms from Seismic Spectra," Phil. Trans. R. Soc. Land. A278, 187-269 (1975).

21. A. R. Edmonds, Angular Momentum in Quantum Mechanics (Princeton University Press, New Jersey, 1960).

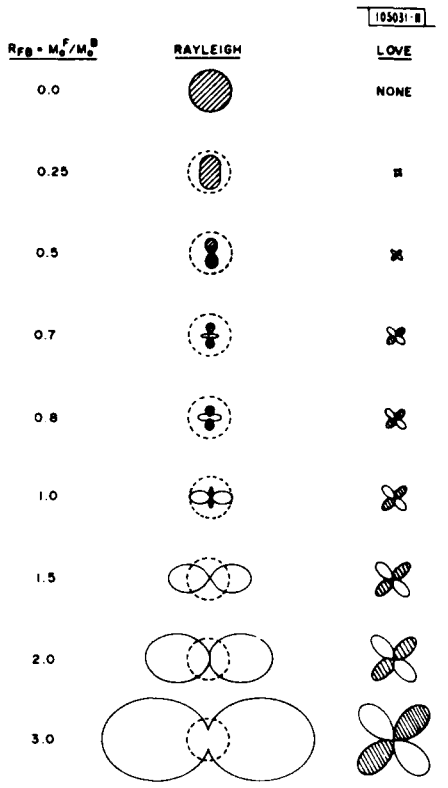

Fig. III-1. Rayleigh- and Love-wave radiation patterns for various combinations of explosive and thrust faulting, expressed as R_{FB}, the ratio of seismic moment of faulting component to that of explosion. Shaded portions denote source phase of −II, unshaded a phase of zero. Dashed circle indicates amplitudes from explosion only. Shape of patterns remains unchanged, increasing in amplitude, as R_{FB} exceeds 3.0.

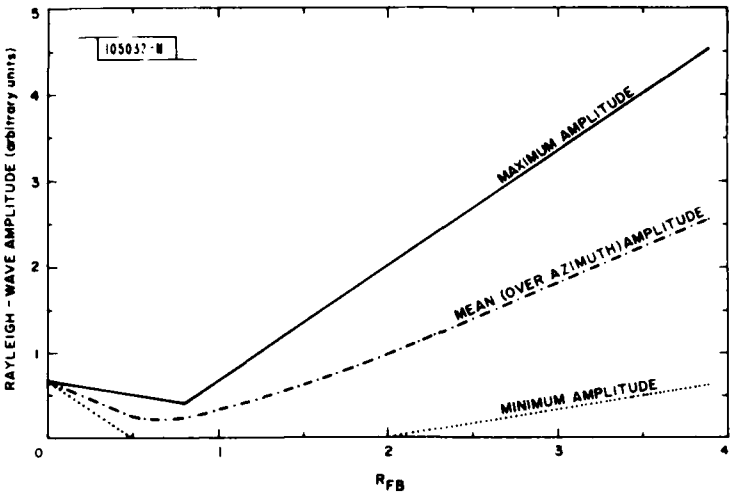

Fig. III-2. Minimum, maximum, and azimuthally averaged Rayleigh-wave spectral amplitudes as a function of R_{FB}.

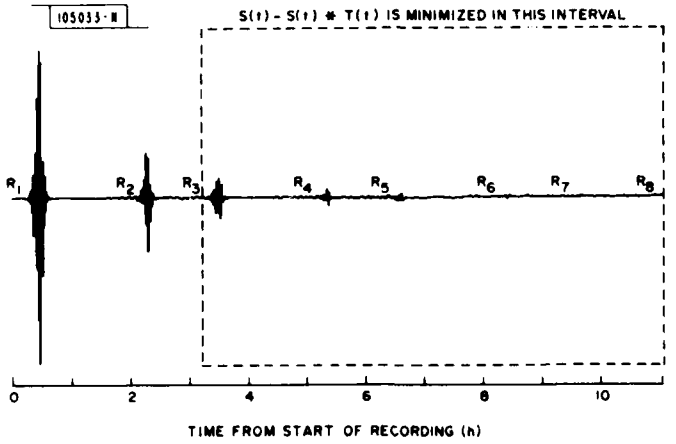

Fig. III-3. Synthetic seismogram for "unknown" structure. Seismogram contains modes of from ${}_0S_2$ to ${}_0S_{97}$; source was at depth of 70 km and receiver at distance of 60° from epicenter. Theoretical seismogram has been convolved with LP WWSSN response and a tapered low-pass filter applied to remove energy at periods shorter than 100 s. Using technique described in this report, we shall derive elements of elastic and anelastic Earth structure that are consistent with information on dispersion and attenuation of surface waves contained in this recording.

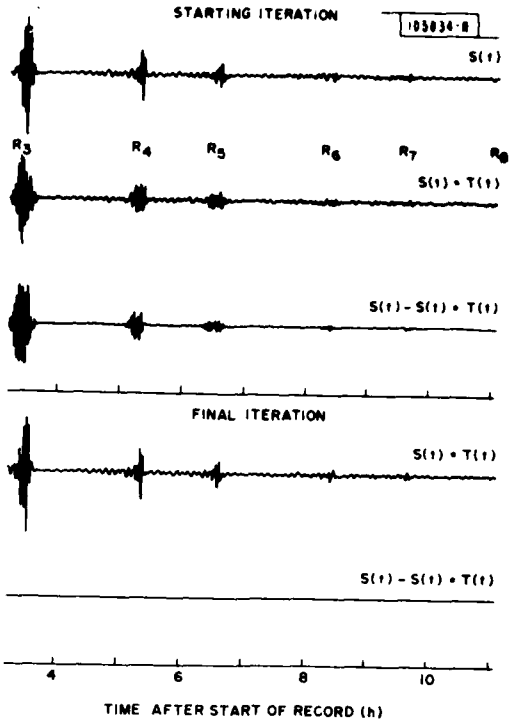

Fig. III-4(a). Top trace is segment of synthetic seismogram shown in Fig. III-3 within area outlined by box. Next trace is truncated result of convolution of seismogram in Fig. III-3 with transfer function T for starting Earth model. If transfer function were consistent with "true" dispersion and attenuation, then third trace would be zero; it clearly is not. However, we improve transfer function in iterative procedure, such that amplitude of difference trace shown at bottom of figure is practically zero.

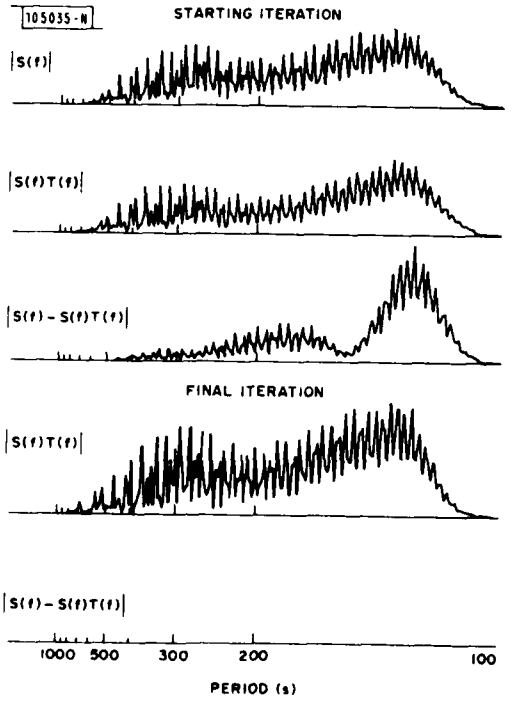

Fig. III-4(b). Frequency-domain representation of information shown in Fig. III-4(a). Only power spectrum is shown.

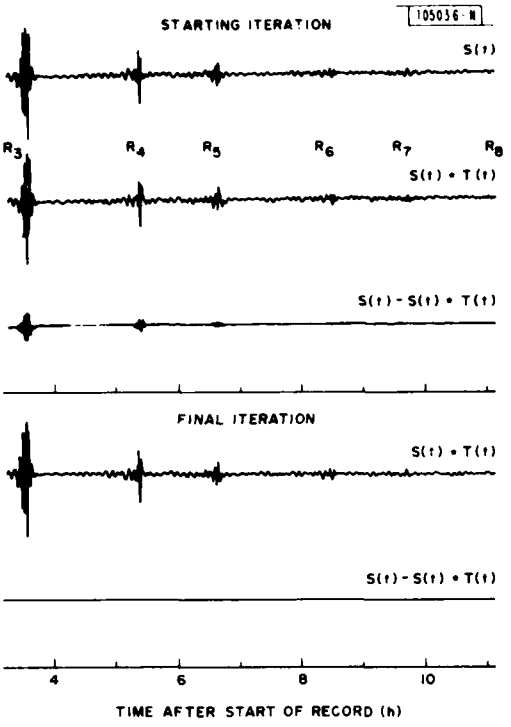

Fig. III-5. Same as Fig. III-4(a) except for improved starting model obtained during first stage (pass) of inversion procedure. Discrepancy between last trace in Fig. III-4(a) and third trace in this figure is result of nonlinear relationship between functionals of a model and perturbations in structural parameters.

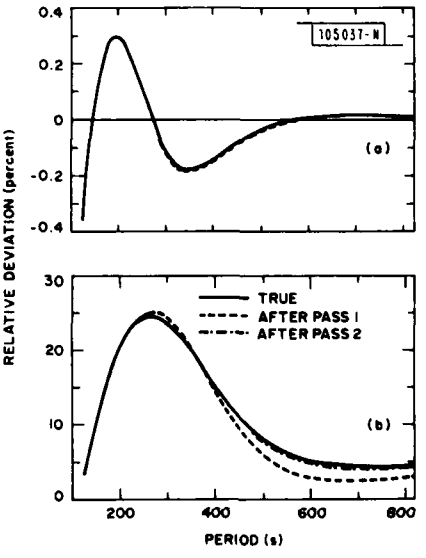

Fig. III-6. Comparison of (a) phase velocities and (b) attenuation, obtained through linearized inversion of waveform data with exact results. Values for starting model represent reference level.

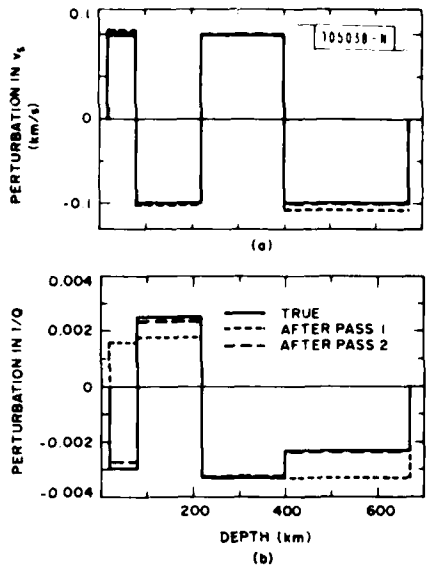

Fig. III-7. Comparison with exact result of (a) shear velocity and (b) shear attenuation profiles retrieved through linearized inversion of waveform data.

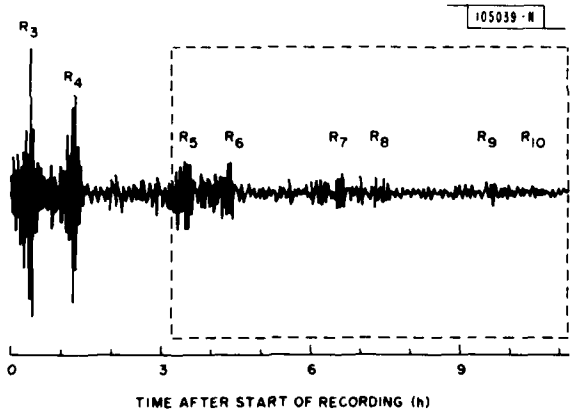

Fig. III-8. Recording of Solomon Islands earthquake of 29 July 1977 by an IDA instrument at Halifax, Nova Scotia. Difference $S(t) - S(t) * T(t)$ is minimized within area outlined by box. Symbols R_n denote individual arrivals of wavegroups of mantle Rayleigh waves.

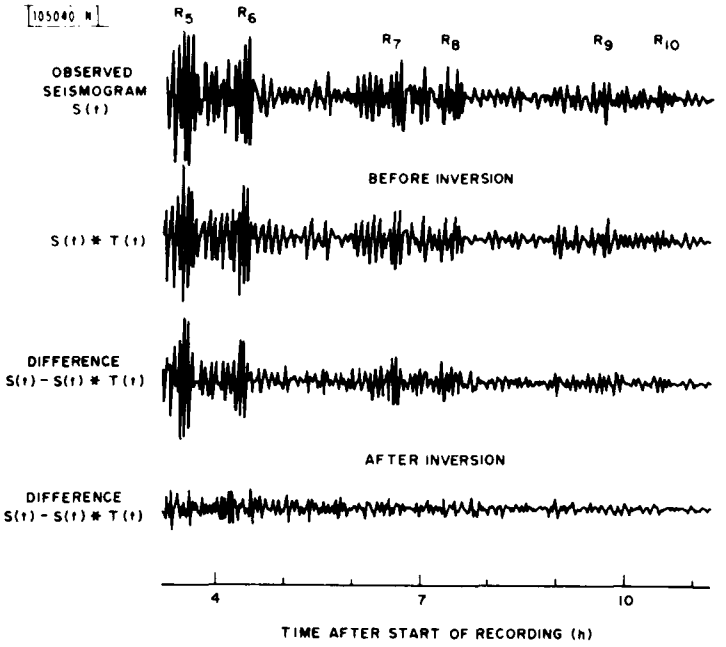

Fig. III-9(a). Top trace is segment of synthetic seismogram shown in Fig. III-8 within area outlined by box. Next trace is truncated result of convolution of seismogram in Fig. III-8 with transfer function T for reference Earth model. Third trace reflects degree of misfit of reference Earth model and structure for particular path; deviations of this magnitude would be observed in source mechanism studies, if excitation kernels are path independent. After structure is "corrected," amplitude of difference trace at bottom of figure is significantly diminished and does not show correlation with arrivals of individual wavegroups.

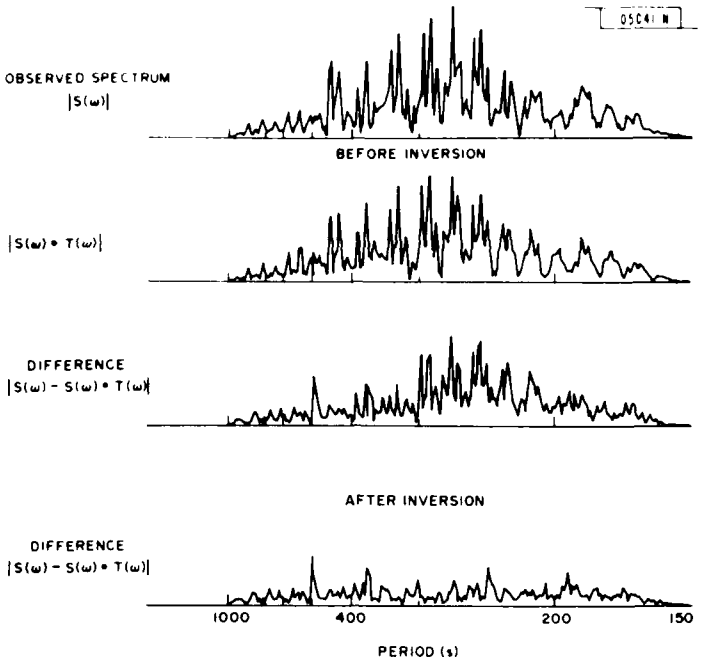

Fig. III-9(b). Frequency-domain representation of Fig. III-9(a); only power spectra are shown. Notice that spectrum of difference trace after inversion appears to be white and that there is no correlation with spectral peaks of fundamental spheroidal mode.

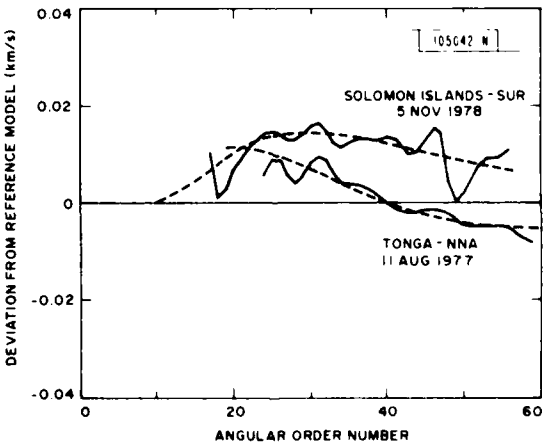

Fig. III-10. Comparison of phase-velocity measurements obtained by linearized inversion technique (LIT) described in report (broken lines) with those derived by traditional phase-delay method (solid lines). Curves obtained by application of LIT are naturally smooth and can easily be differentiated to obtain group velocities, for example.

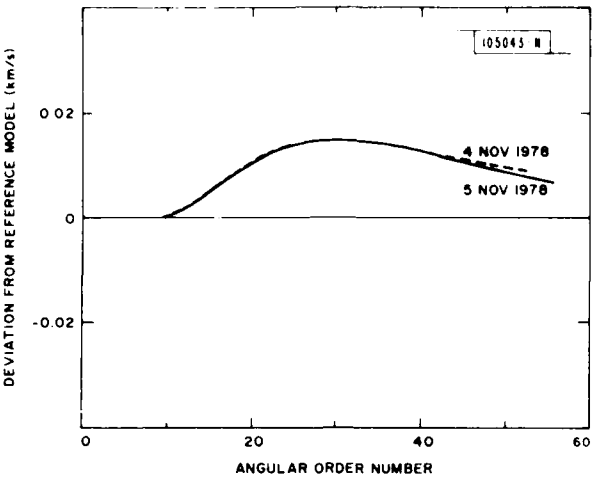

Fig. III-11. Repeatability of measurements is demonstrated by results of measurements performed on recordings of two earthquakes of nearly identical location and similar source mechanism.

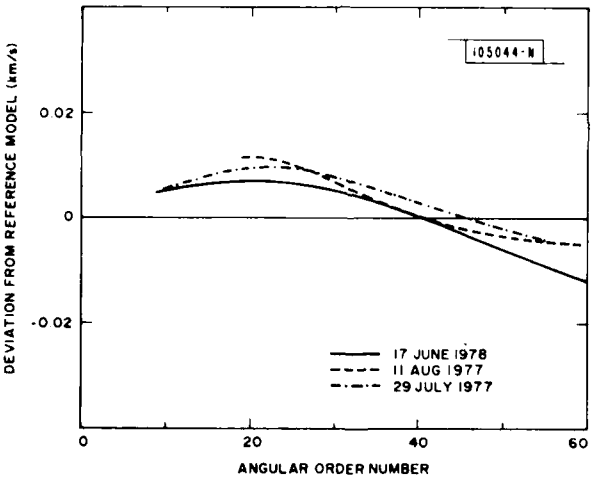

Fig. III-12. Measurements for three earthquakes recorded at Naña, Peru. Great-circle paths were nearly identical (their poles are within 100 km of each other), but epicenters were in different seismic zones (Tonga, New Guinea, and Japan) and source mechanisms were most likely different. Woodhouse (Sec. D, this issue) shows that for a given great-circle path and a fixed receiver, observed period of free oscillation depends, in general, on position of source and its mechanism.

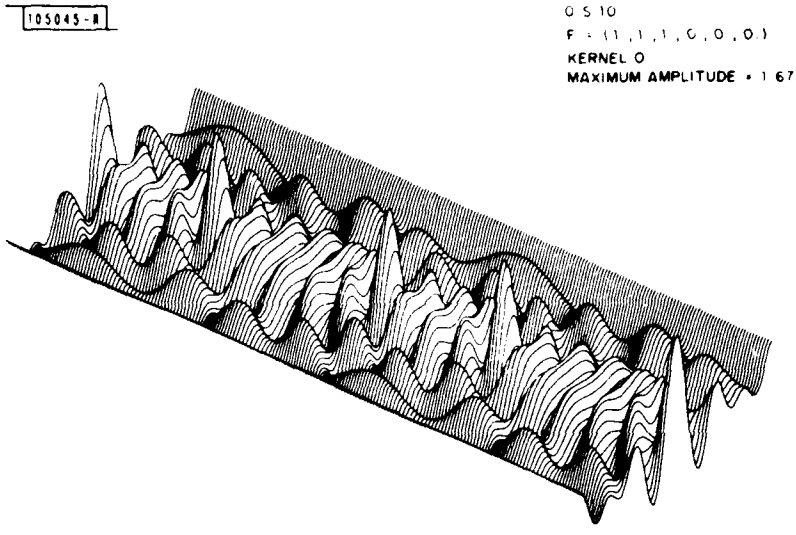

(a)

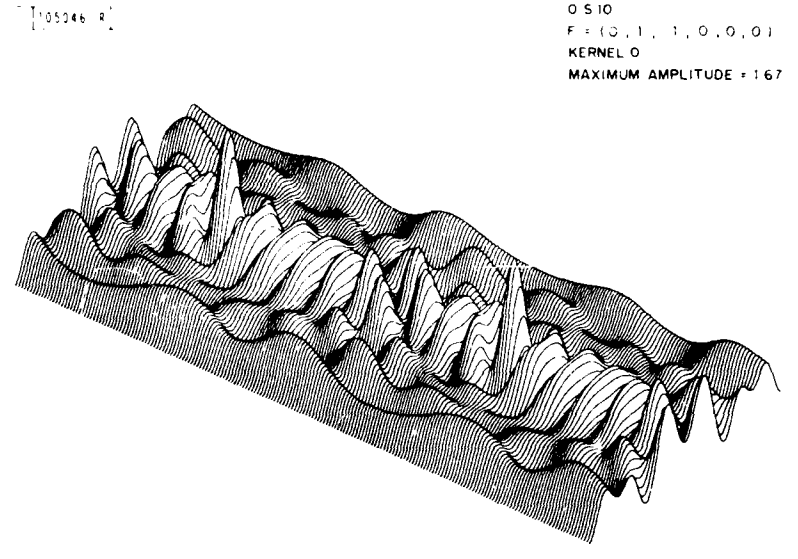

(b)

Fig. III-13(a-c). Shown, in a three-dimensional representation, are kernels by which fundamental spheroidal modes sample lateral heterogeneity of Earth. Horizontal plane represents a Mercator projection of Earth's surface, with equator running longitudinally. A source and a receiver lie on equator, a distance 108° apart, at points indicated by two rightmost peaks in (a) and (c). (a) and (b) differ only in source mechanism, and, though their largest differences are close to source, they differ appreciably throughout Earth.

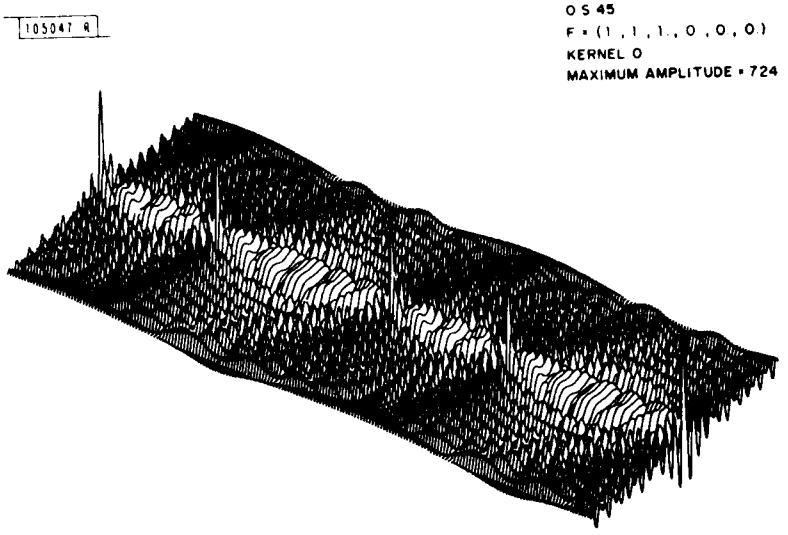

(c)

Fig. III-13(a-c). *Continued.*

GLOSSARY

ASRO	Upgraded HGLP Station, with Digital Recording
BTL	Bell Telephone Laboratories
CATV	Cable Access Television
CD	Committee on Disarmament
CLVD	Compensated Linear Vector Dipole
DARPA	Defense Advanced Research Projects Agency
DEC	Digital Equipment Corporation
DMA	Direct Memory Access
DOE	Department of Energy
EDR	Earthquake Data Reports
FIFO	First In, First Out
FSCD	Function Switches and Control Dials Module
HGLP	High Gain Long Period
IDA	International Deployment of Accelerometers
I/O	Input-Output
ISC	International Seismological Center
J-B	Jeffreys-Bullen
JMA	Japan Meteorological Agency
LIT	Linearized Inversion Technique
LP	Long Period
LPZ	Long Period, Vertical Component
NMRD	DARPA Nuclear Monitoring Research Division
NSS	National Seismic Stations
NTS	Nevada Test Site
PDE	Preliminary Determination of Epicenters
RMS	Root Mean Square
SAS	Seismic Analysis Station
SATS	Semiannual Technical Summary
SDC	Seismic Data Center
SP	Short Period
SPZ	Short Period, Vertical Component
SRO	Seismic Research Observatory

TUNE	Modified UNIX Kernel
UNIX	UNIX Operating System (UNIX is a Trademark of Bell Laboratories)
VHF	Very High Frequency
WWSSN	World-Wide Standard Seismograph Network

UNCLASSIFIED

SECURITY CLASSIFICATION OF THIS PAGE (When Data Entered)

REPORT DOCUMENTATION PAGE	READ INSTRUCTIONS BEFORE COMPLETING FORM
1. REPORT NUMBER: ESD-TR-80-191	2. GOVT ACCESSION NO.: AD-A097999
	3. RECIPIENT'S CATALOG NUMBER
4. TITLE (and Subtitle): Seismic Discrimination	5. TYPE OF REPORT & PERIOD COVERED: Semiannual Technical Summary, 1 April – 30 September 1980
	6. PERFORMING ORG. REPORT NUMBER
7. AUTHOR(s): Michael A. Chinnery	8. CONTRACT OR GRANT NUMBER(s): F19628-80-C-0002
9. PERFORMING ORGANIZATION NAME AND ADDRESS: Lincoln Laboratory, M.I.T., P.O. Box 73, Lexington, MA 02173	10. PROGRAM ELEMENT, PROJECT, TASK AREA & WORK UNIT NUMBERS: ARPA Order-512, Program Element No. 61101E, Project No. 0D60
11. CONTROLLING OFFICE NAME AND ADDRESS: Defense Advanced Research Projects Agency, 1400 Wilson Boulevard, Arlington, VA 22209	12. REPORT DATE: 30 September 1980
	13. NUMBER OF PAGES: 76
14. MONITORING AGENCY NAME & ADDRESS (if different from Controlling Office): Electronic Systems Division, Hanscom AFB, Bedford, MA 01731	15. SECURITY CLASS. (of this report): Unclassified
	15a. DECLASSIFICATION DOWNGRADING SCHEDULE

16. DISTRIBUTION STATEMENT (of this Report)

Approved for public release; distribution unlimited.

17. DISTRIBUTION STATEMENT (of the abstract entered in Block 20, if different from Report)

18. SUPPLEMENTARY NOTES

None

19. KEY WORDS (Continue on reverse side if necessary and identify by block number)

seismic discrimination
seismic array
seismology
surface waves
body waves
LASA
NORSAR
ARPANET

20. ABSTRACT (Continue on reverse side if necessary and identify by block number)

This Semiannual Technical Summary describes the Lincoln Laboratory Vela Uniform program for the period 1 April to 30 September 1980. Section I describes progress in the development of a prototype Seismic Data Center. During this report period, advances have been made in three important subsystems: the Seismic Analysis Station, the Local Computer Network, and the Data Base Management System. Section II describes a series of studies into the seismic processing algorithms to be used at the Seismic Data Center. The results of several investigations in General Seismology are included in Sec. III.

DD FORM 1 JAN 73 1473 EDITION OF 1 NOV 65 IS OBSOLETE

UNCLASSIFIED

SECURITY CLASSIFICATION OF THIS PAGE (When Data Entered)

207650